W samples (9/20, 45%) and 6 were *cagA* positive in EW samples (6/48, 13%). We did not find any correlation between *ureA*- or *cagA*-positive detection and DNA methylation.

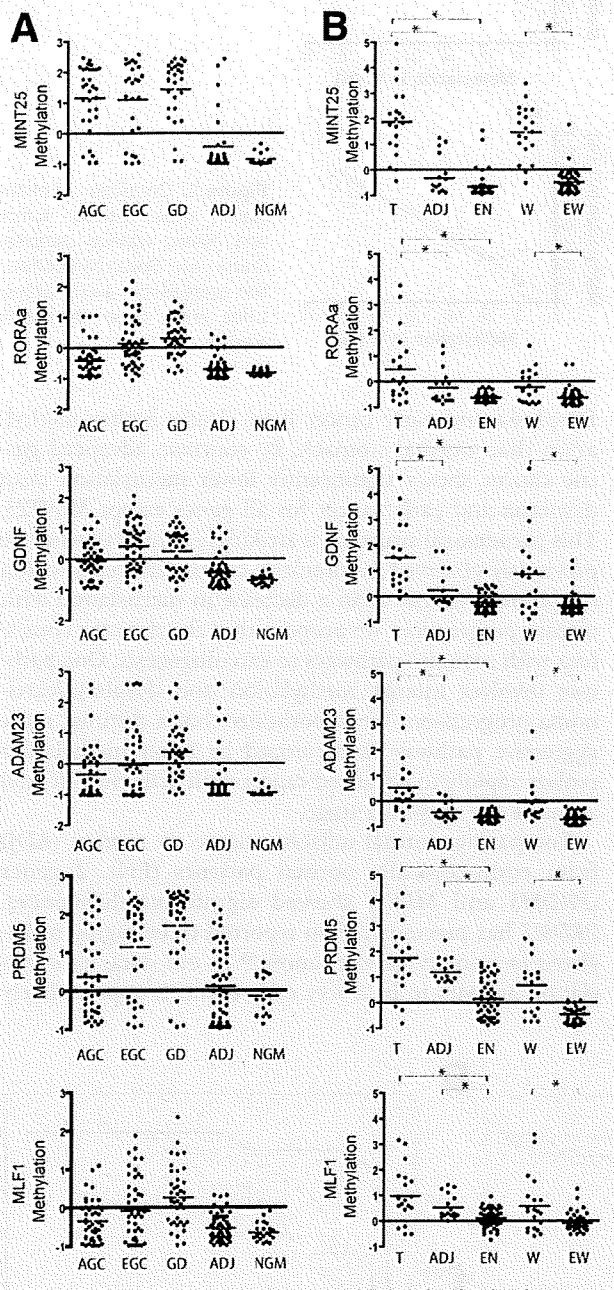

Figure 1. Methylation in gastric cancer. Methylation levels of 6 genes (*MINT25*, *RORAa*, *GDNF*, *ADAM23*, *PRDM5*, and *MLF1*) was measured by bisulfite pyrosequencing and normalized by the *z* score method. (*A*) Results of individual genes in the test set. (*B*) Results of individual genes in the validation set. EGC, early gastric cancer; AGC, advanced gastric cancer; GD, gastric dysplasia; NGM, nonneoplastic gastric mucosa; T, tumor tissue in patient with gastric cancer; ADJ, normal adjacent tissue to tumors; W, stomach wash sample in patient with gastric cancer; EN, stomach mucosal tissue in endoscopically normal patient; EW, stomach wash sample in endoscopically normal patient (*$P < .05$).

Discussion

Gastric cancer is still a lethal disease around the world. Early detection yields the opportunity for less-invasive curative treatment and may improve prognosis. Some detection tools are currently being used such as fluoroscopy, endoscopy, and tumor markers; however, these tools lack sensitivity and may require invasive techniques.[34] Alternatively, serum DNA methylation can be used as a marker; however, it provides only a narrow range of sensitivity.[35] Using stool DNA is not useful for gastric cancer detection because of DNA damage because of stomach acidity and the length of the GI tract. Here, we have identified sensitive markers of early gastric cancer, and we developed a new method of gastric cancer detection with the use of methylation analysis of gastric washes.

The use of stomach juice as a molecular diagnostic or prediction tool has been previously shown to be unfeasible because DNA is easily denatured by gastric acidity. Therefore, it is important to obtain genomic DNA from fresh cells not affected by stomach acidity. Our data show that gastric washes can yield enough DNA from shed epithelium to be used for the screening and detection of gastric cancer and that methylation analysis in this compartment confers a high sensitivity and specificity.

We found a close correlation between methylation levels in biopsy and wash samples. Our data suggest that cancer cells from the mucosal layer are easily exfoliated into gastric washes, possibly because of loosening cell-to-cell junctions, whereas the exfoliation of normal mucosal cells is limited. In addition, the success of the technique may relate to the fact that, normally, DNA recovered from gastric washes is relatively degraded. In patients with cancer, a significant proportion of the DNA derives from exfoliated cells, is of larger molecular weight, is less degraded through the apoptotic process, and is easier to amplify by PCR; therefore; its methylation reflects well that of the tumors (Supplementary Figures 5 and 6). Therefore, we can obtain a larger fraction of cancer cells than normal cells in the washes, even if the area of the cancer site is smaller than that of the normal mucosa. Indeed, our approach was successful, although the washes were not specifically directed at diseased parts of the stomach. These data raise the hope that gastric washes without requiring an endoscope may also be successful in cancer detection, an approach that should be tested in future trials.

We identified 6 frequently methylated genes in gastric neoplasia that can serve as biomarkers for the disease. Methylation changes of these markers during gastric carcinogenesis are gene and tumor stage dependent. Of these genes, *MINT25* and *GDNF* were stable biomarkers, because they were highly methylated in gastric tumor samples irrespective of tumor stage. The 6 genes were already reported to be densely methylated in gastric cancer except for *GDNF*.[36,37] For 5 genes (*AMAD23*, *PRDM5*,

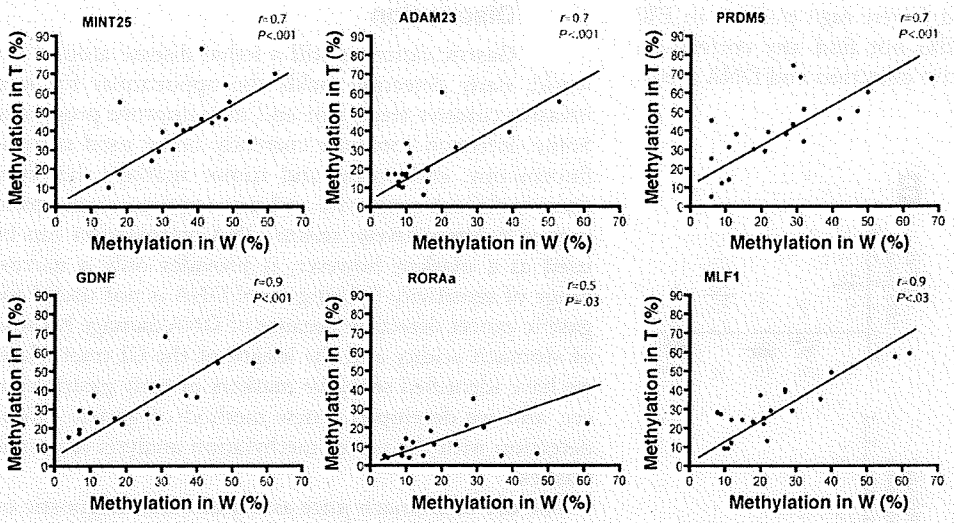

Figure 2. Correlation of methylation levels between tumor and gastric washes samples. Shown are Spearman correlation coefficients *r* and *P* values. Lines show linear regression models.

GDNF, RORA, MLF1), we showed correlations between expression and methylation. For *MINT25*, this was not shown, because it corresponds to an alternate promoter of the *CABIN1* gene. Our data do not address whether these genes are functionally involved in gastric neoplasia, but this criterion is not necessary for cancer detection.

Of the genes we studied, *MINT25* had the best sensitivity (90%), specificity (96%), and area under the ROC curve (0.961) in terms of tumor detection. A combination of individual genes in methylation panels could increase the performance of these markers: *MINT25* + *ADAM23* + *GDNF* (sensitivity, 95%; specificity, 92%; area under the ROC curve, 0.965; positive predictive value, 0.83; negative predictive value, 0.98). The panel of *MINT25* + *ADAM23* + *GDNF* had greater sensitivity than did *MINT25* alone (Table 3); thus, it may be better for screening. It will be important to validate gene combinations in separate data sets, however.

In this study, we found surprising differences in DNA methylation between different stages of gastric cancer. Dysplasia and early cancer have clearly higher methylation than normal stomach. By contrast, advanced gastric cancer shows significantly lower methylation than dysplasia and early cancer for all genes except *MINT25*. This paradoxical situation is strikingly similar to what we previously observed in ulcerative colitis–associated colon neoplasia.[33] Rather than a decrease in methylation with disease progression, we propose that the data are consistent with separate pathways to carcinogenesis. One pathway involves intense methylation and dysplasia/carcinoma progression. We hypothesize that a distinct, more aggressive pathway characterized by lower methylation evolves rapidly to advanced cancer with little time (if any) spent at the dysplasia stage.

Comparing normal adjacent tissue to tumors (ADJ) from endoscopically normal patients (EN), 2 genes (*PRDM5* and *MLF1*) showed significant differences. *PRDM5* has previously been reported to be highly methylated in primary gastric cancer.[38] In our data, its methylation appears to be a very early event. It appears likely

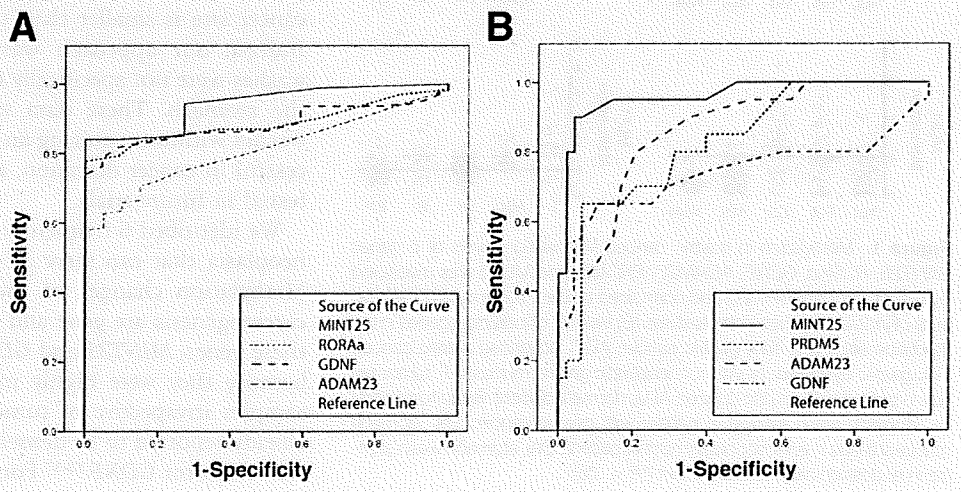

Figure 3. Receiver operating characteristic (ROC) curves for methylation-based detection of gastric cancer. The *z* score of DNA methylation in test (*A*) and validation (*B*) sets were plotted with the use of the top 4 candidate genes in each (test set: *MINT25*, *RORAa*, *GDNF*, *ADAM23*; validation set: *MINT25*, *ADAM23*, *PRDM5*, *GDNF*).

Table 3. Performance of Gene Markers for the Detection of Gastric Neoplasia

A. Test set (cancer versus normal)

Marker	Area (SE)	Cutoff (*z* score)	Neoplasm		Normal		Sensitivity (%)	Specificity (%)	PPV	NPV
			Positive	Total	Positive	Total				
MINT25	0.943 (0.025)	−0.4541	75	88	1	15	84.1	90.9	.99	.52
RORAa	0.887 (0.026)	−0.7135	114	131	8	22	83.2	86.4	.93	.45
GDNF	0.884 (0.027)	−0.4911	104	127	2	22	81.9	90.9	.98	.47
ADAM23	0.812 (0.036)	−0.7876	83	126	2	20	65.9	90.0	.98	.30
PRDM5	0.754 (0.042)	0.5094	68	106	1	19	64.2	94.7	.99	.32
MLF1	0.727 (0.040)	−0.4170	81	131	4	22	61.8	81.8	.95	.26

B. Validation set (gastric washes in cancer patients versus controls)

Variable	Area (SE)	Cutoff (*z* score)	W		EW		Sensitivity (%)	Specificity (%)	PPV	NPV
			Positive	Total	Positive	Total				
MINT25	0.961 (0.025)	0.0571	18	20	2	48	90.0	95.8	.90	.96
RORAa	0.707 (0.076)	−0.4213	11	19	7	48	60.0	85.4	.61	.84
GDNF	0.740 (0.083)	0.0285	13	20	5	47	65.0	89.6	.72	.86
ADAM23	0.864 (0.047)	−0.4949	13	19	8	48	70.0	83.3	.62	.87
PRDM5	0.827 (0.054)	0.0939	13	20	3	48	65.0	93.7	.81	.87
MLF1	0.678 (0.089)	0.2411	12	20	7	48	60.0	85.4	.63	.84
MINT25 + PRDM5 + ADAM23	0.963 (0.020)	−0.6015	18	20	4	48	90.0	91.7	.82	.96
MINT25 + ADAM23 + GDNF	0.965 (0.020)	−0.8141	19	20	4	48	95.0	91.7	.83	.98

EW, gastric wash in cancer-free controls; NPV, negative predictive value; PPV, positive predictive value; SE indicates standard error; W, gastric wash in patients with cancer.

that these 2 genes are associated with field cancerization,[22] and it would be interesting to determine prospectively whether this methylation can be found in "at risk" populations before cancer development.

DNA methylation analysis can be a useful biomarker of cancer, but it is important to consider detection methods. Pyrosequencing is a cost- and time-effective assay that provides quantitative screening. This allows one to set cutoff points, which makes accurate comparisons possible, and overcomes some of the problems associated with very sensitive bisulfite DNA amplification methods. Its applicability however is limited to situations in which the tissue/DNA to be studied has a high fraction of tumor cells.

In summary, we identified 6 methylation markers for detection of early gastric neoplasia, 2 of which could be useful as markers of the field cancerization. Moreover, we have developed a new method for gastric cancer detection by DNA methylation analysis in gastric washes. This technology should now be tested in prospective studies for evaluation and detection of gastric cancer.

Supplementary Data

Note: To access the supplementary material accompanying this article, visit the online version of *Gastroenterology* at www.gastrojournal.org, and at doi: 10.1053/j.gastro.2009.02.085.

References

1. Hohenberger P, Gretschel S. Gastric cancer. Lancet 2003;362:305–315.
2. Parkin DM. Global cancer statistics in the year 2000. Lancet Oncol 2001;2:533–543.
3. Jemal A, Siegel R, Ward E, et al. Cancer statistics, 2008. CA Cancer J Clin 2008;58:71–96.
4. Denk H, Tappeiner G, Davidovits A, Holzner HJ. The carcinoembryonic antigen (CEA) in carcinomata of the stomach. Virchows Arch A Pathol Pathol Anat 1973;360:339–347.
5. Koprowski H, Steplewski Z, Mitchell K, Herlyn M, Herlyn D, Fuhrer P. Colorectal carcinoma antigens detected by hybridoma antibodies. Somatic Cell Genet 1979;5:957–971.
6. Feltus FA, Lee EK, Costello JF, Plass C, Vertino PM. Predicting aberrant CpG island methylation. Proc Natl Acad Sci U S A 2003;100:12253–12258.
7. Ushijima T, Sasako M. Focus on gastric cancer. Cancer Cell 2004;5:121–125.
8. Horii A, Nakatsuru S, Miyoshi Y, et al. The APC gene, responsible for familial adenomatous polyposis, is mutated in human gastric cancer. Cancer Res 1992;52:3231–3233.
9. Nanus DM, Kelsen DP, Mentle IR, Altorki N, Albino AP. Infrequent point mutations of ras oncogenes in gastric cancers. Gastroenterology 1990;98:955–960.
10. Maesawa C, Tamura G, Suzuki Y, et al. The sequential accumulation of genetic alterations characteristic of the colorectal adenoma-carcinoma sequence does not occur between gastric adenoma and adenocarcinoma. J Pathol 1995;176:249–258.
11. Laird PW. The power and the promise of DNA methylation markers. Nat Rev Cancer 2003;3:253–266.
12. Issa JP. CpG island methylator phenotype in cancer. Nat Rev Cancer 2004;4:988–993.
13. Ushijima T. Detection and interpretation of altered methylation patterns in cancer cells. Nat Rev Cancer 2005;5:223–231.

14. Belinsky SA, Klinge DM, Dekker JD, et al. Gene promoter methylation in plasma and sputum increases with lung cancer risk. Clin Cancer Res 2005;11:6505–6511.
15. Itzkowitz SH, Jandorf L, Brand R, et al. Improved fecal DNA test for colorectal cancer screening. Clin Gastroenterol Hepatol 2007; 5:111–117.
16. Suzuki H, Toyota M, Sato H, Sonoda T, Sakauchi F, Mori M. Roles and causes of abnormal DNA methylation in gastrointestinal cancers. Asian Pac J Cancer Prev 2006;7:177–185.
17. Kusano M, Toyota M, Suzuki H, et al. Genetic, epigenetic, and clinicopathologic features of gastric carcinomas with the CpG island methylator phenotype and an association with Epstein-Barr virus. Cancer 2006;106:1467–1479.
18. Issa JP, Shen L, Toyota M. CIMP, at last. Gastroenterology 2005; 129:1121–1124.
19. Toyota M, Ohe-Toyota M, Ahuja N, Issa JP. Distinct genetic profiles in colorectal tumors with or without the CpG island methylator phenotype. Proc Natl Acad Sci U S A 2000;97:710–715.
20. Toyota M, Ahuja N, Suzuki H, et al. Aberrant methylation in gastric cancer associated with the CpG island methylator phenotype. Cancer Res 1999;59:5438–5442.
21. Toyota M, Ahuja N, Ohe-Toyota M, Herman JG, Baylin SB, Issa JP. CpG island methylator phenotype in colorectal cancer. Proc Natl Acad Sci U S A 1999;96:8681–8686.
22. Shen L, Kondo Y, Rosner GL, et al. MGMT promoter methylation and field defect in sporadic colorectal cancer. J Natl Cancer Inst 2005;97:1330–1338.
23. Dakubo GD, Jakupciak JP, Birch-Machin MA, Parr RL. Clinical implications and utility of field cancerization. Cancer Cell Int 2007;7:2.
24. Kim SK, Jang HR, Kim JH, et al. The epigenetic silencing of LIMS2 in gastric cancer and its inhibitory effect on cell migration. Biochem Biophys Res Commun 2006;349:1032–1040.
25. Ferrini AM, Mannoni V, Pontieri E, Pourshaban M. Longer resistance of some DNA traits from BT176 maize to gastric juice from gastrointestinal affected patients. Int J Immunopathol Pharmacol 2007;20:111–118.
26. Colella S, Shen L, Baggerly KA, Issa JP, Krahe R. Sensitive and quantitative universal Pyrosequencing methylation analysis of CpG sites. Biotechniques 2003;35:146–150.
27. Rhei E, Bogomolniy F, Federici MG, et al. Molecular genetic characterization of BRCA1- and BRCA2-linked hereditary ovarian cancers. Cancer Res 1998;58:3193–3196.
28. Qin T, Youssef EM, Jelinek J, et al. Effect of cytarabine and decitabine in combination in human leukemic cell lines. Clin Cancer Res 2007;13:4225–4232.
29. Clayton CL, Kleanthous H, Coates PJ, Morgan DD, Tabaqchali S. Sensitive detection of Helicobacter pylori by using polymerase chain reaction. J Clin Microbiol 1992;30:192–200.
30. Smith SI, Oyedeji KS, Arigbabu AO, et al. Comparison of three PCR methods for detection of Helicobacter pylori DNA and detection of cagA gene in gastric biopsy specimens. World J Gastroenterol 2004;10:1958–1960.
31. Estecio MR, Yan PS, Ibrahim AE, et al. High-throughput methylation profiling by MCA coupled to CpG island microarray. Genome Res 2007;17:1529–1536.
32. Chung W, Kwabi-Addo B, Ittmann M, et al. Identification of novel tumor markers in prostate, colon and breast cancer by unbiased methylation profiling. PLoS ONE 2008;3:e2079.
33. Konishi K, Shen L, Wang S, Meltzer SJ, Harpaz N, Issa JP. Rare CpG island methylator phenotype in ulcerative colitis-associated neoplasias. Gastroenterology 2007;132:1254–1260.
34. Posner MR, Mayer RJ. The use of serologic tumor markers in gastrointestinal malignancies. Hematol Oncol Clin North Am 1994;8:533–553.
35. Koike H, Ichikawa D, Ikoma H, Otsuji E, Kitamura K, Yamagishi H. Comparison of methylation-specific polymerase chain reaction (MSP) with reverse transcriptase-polymerase chain reaction (RT-PCR) in peripheral blood of gastric cancer patients. J Surg Oncol 2004;87:182–186.
36. Takada H, Imoto I, Tsuda H, et al. ADAM23, a possible tumor suppressor gene, is frequently silenced in gastric cancers by homozygous deletion or aberrant promoter hypermethylation. Oncogene 2005;24:8051–8060.
37. Yamashita S, Tsujino Y, Moriguchi K, Tatematsu M, Ushijima T. Chemical genomic screening for methylation-silenced genes in gastric cancer cell lines using 5-aza-2′-deoxycytidine treatment and oligonucleotide microarray. Cancer Sci 2006;97:64–71.
38. Watanabe Y, Toyota M, Kondo Y, et al. PRDM5 identified as a target of epigenetic silencing in colorectal and gastric cancer. Clin Cancer Res 2007;13:4786–4794.

Received March 24, 2008. Accepted February 26, 2009.

Reprint requests

Address requests for reprints to: Jean-Pierre J. Issa, MD, Department of Leukemia, The University of Texas M.D. Anderson Cancer Center, 1515 Holcombe Boulevard, Unit 428, Houston, TX 77030. e-mail: jpissa@mdanderson.org; fax: (713) 745-2261.

Acknowledgments

Y.W. and H.S.K. contributed equally to this work.

Conflicts of interest

The authors disclose no conflicts.

Funding

This work was supported in part by the National Institutes of Health grants CA098006 and CA105346. J.-P.J.I. is an American Cancer Society Clinical Research Professor supported by a generous gift from the F.M. Kirby Foundation. H.-S.K. was supported by grant 2006-070-C00031 from the Korea Research Foundation and an intramural grant-in-aid from Yonsei University Wonju College of Medicine (2006). DNA sequencing in the Core Sequencing facility at the M.D. Anderson Cancer Center is supported by Core Grant CA16672 from the National Institutes of Health.

Global DNA hypomethylation suppresses squamous carcinogenesis in the tongue and esophagus

Seiji Baba,[1,2] Yasuhiro Yamada,[1,3,4] Yuichiro Hatano,[1] Yasuo Miyazaki,[1,2] Hideki Mori,[1] Toshiyuki Shibata[2] and Akira Hara[1]

Departments of [1]Tumor Pathology, [2]Oral and Maxillofacial Sciences, Gifu University Graduate School of Medicine, Gifu; [3]PRESTO, Japan Science and Technology Agency, Saitama, Japan

(Received February 2, 2009/Revised March 17, 2009/Accepted March 17, 2009/Online publication April 21, 2009)

Genome-wide DNA hypomethylation and concomitant site-specific gene hypermethylation are among the most common molecular alterations in human neoplasia. Previous studies revealed that genetic reduction of the DNA methylation level results in opposing effects on tumor development, depending on the tumor cell type and on the different stages of the tumorigenesis. For instance, reduced levels of DNA methylation in mice strongly inhibited tumor development of the intestine, whereas they induced thymic lymphomas and liver tumors. In the present study, using DNA methyltrasferase 1 (*Dnmt1*) hypomorphic alleles to reduce genomic methylation, we examined the effects of DNA hypomethylation on a murine squamous carcinogenesis in the tongue and esophagus induced by 4-nitroquinoline 1-oxide. Genetic reduction of DNA methylation level led to the suppression of tumor formation in both tongue and esophagus. Histological analyses revealed that DNA hypomethylation preferentially inhibited the development of squamous cell carcinomas. The results suggest that genomic hypomethylation inhibits squamous carcinogenesis in the tongue and esophagus, and that pharmacological modification of epigenetic status might be useful for the prevention and treatment of cancers in the upper digestive tract. (*Cancer Sci* 2009; 100: 1186–1191)

Altered DNA methylation in the form of global hypomethylation and regional hypermethylation is one of the most consistent epigenetic changes in cancer.[1] Global DNA hypomethylation, which is frequently observed at early stages of tumorigenesis in human cancer, promotes tumor development in mouse models and causes chromosomal instability in cultured fibroblasts.[2] After the initial observation of DNA hypermethylation within the retinoblastoma tumor suppressor gene, a number of genes have been shown to be hypermethylated and transcriptionally silenced in tumors. Although the consequences of global hypomethylation and gene-specific hypermethylation have been mechanistically connected to chromosome instability and transcriptional silencing, respectively,[3–5] the causes of aberrant genomic methylation patterns are currently unknown.

DNA methylation is catalyzed by a family of three DNA methyltransferases: Dnmt1, Dnmt3a, and Dnmt3b.[6–8] Although the three Dnmt partially cooperate to establish and maintain genomic methylation patterns, they also have distinctive functions. Dnmt1 has a preference for hemimethylated DNA, and indeed a hypomorphic allele of Dnmt1 has been shown to cause global DNA hypomethylation. Thus, Dnmt1 is considered to be the major maintenance methyltransferase. Using *Dnmt1* hypomorphic alleles as a model for global DNA hypomethylation, previous studies have revealed that global DNA hypomethylation inhibits tumorigenesis in the intestine,[5] whereas it induces or promotes T-cell lymphomas,[9] liver cancers,[4] and fibrosarcomas.[10] These results indicate that the forced reduction of genomic methylation levels leads to opposing effects on tumorigenesis depending on the cell type. Considering the fact that DNA hypomethylating agents have been used for cancer therapy in a subset of cancer,[1] it is important to clarify the effect of global DNA hypomethylation on the risk for tumor development in various organs.

The potent carcinogenicity of 4-nitroquinoline 1-oxide (4NQO) depends on the formation of DNA adducts, in addition to the exertion of oxidative stress in target cells.[11,12] 4NQO has been shown to produce squamous neoplasms preferentially in the tongue and a small number of tumors arise in the esophagus in rodents exposed to 4NQO.[13,14] There is a histological sequence of epithelial changes from dysplasia through invasive squamous cell carcinoma (SCC) in this model.[14] In the present study, we have investigated the effect of reduced DNA methylation levels on the squamous cell carcinogenesis induced by 4NQO and found that global DNA hypomethylation can suppress the tumorigenesis in both the tongue and esophagus.

Materials and Methods

Mice. All animal studies and breeding were carried out under the Regulations for Animal Experiments in Gifu University. Two mutant alleles of *Dnmt1* were used: the null $Dnmt1^{c}$ allele in the C57BL/6 background[15] and the hypomorphic $Dnmt1^{chip}$ allele in the 129Sv4 background.[9] $Dnmt1^{c/+}$ mice were crossed with female $Dnmt1^{chip/chip}$ mice (129Sv4) to generate all experimental mice in an isogenic F_1 hybrid (C57 : 129) background. Previous study indicated that $Dnmt1^{chip/+}$ mice have the same levels of genomic methylation as $Dnmt1^{+/+}$ mice, whereas $Dnmt1^{chip/c}$ mice have reduced DNA methylation contents at pricentromeric satellite repeats.[4] Therefore, we analyzed 28 $Dnmt1^{chip/+}$ mice as a control cohort, and 28 $Dnmt1^{chip/c}$ mice as a DNA hypomethylated cohort to quantify both the tongue and esophagus lesions at 25 weeks of age. Tumors were quantified along the surface of the tissue, and were further analyzed after dissection.

4NQO exposure. A total of 56 mice were used for the studies with 4NQO. We used both male and female mice in the present study. All mice were maintained under specific pathogen-free conditions with isolated ventilation cages in an air-conditioned room with a 12 : 12 L : D cycle. They were bred and maintained on a basal diet, CE-2 (CLEA Japan, Tokyo, Japan) until termination of the study. Genotypes were identified by PCR analysis of tail DNA using allele-specific primers. The mice were administrated with drinking water containing 4NQO at concentrations of 0.1 mg/mL (23 $Dnmt1^{chip/+}$ mice and 22 $Dnmt1^{chip/c}$ mice) or no 4NQO (five $Dnmt1^{chip/+}$ mice and six $Dnmt1^{chip/c}$ mice), starting at 5 weeks of age until the termination of the experiment. To examine tongue and esophagus lesions, 25-week-old $Dnmt1^{chip/c}$ and age-matched $Dnmt1^{chip/+}$ littermates

[4]To whom correspondence should be addressed. E-mail: y-yamada@gifu-u.ac.jp

doi: 10.1111/j.1349-7006.2009.01171.x

were killed. As reported previously,[9] we observed a decreased bodyweight in *Dnmt1*$^{chip/c}$ mice in comparison with *Dnmt1*$^{chip/+}$ littermates.[9] However, there was no detectable difference in consumption of the drinking water containing 4NQO (data not shown).

Preparation of tissue samples for tumor counting and histological analysis. All mice underwent a thorough postmortem examination at the time of death. The tongue and esophagus were removed and the esophagus was opened along the longitudinal axis. The number as well as the longest diameter of the tumors in the tongue and esophagus were measured using a dissecting microscope. Tumors >0.5 mm in diameter were mapped and counted. To eliminate interobserver error, all counts were done by a single observer blinded to the genotype of the mice. All of the cases were also counted by a second observer to confirm the results of the first observer. After tumor counting, the tongues were cut at the longitudinal center and were processed for the assessment of microscopic lesions. The incidences and multiplicities of microscopic lesions in the tongue were determined on histological sections at the longitudinal center of the tongue. In contrast to the tongue tumors, all esophageal tumors were processed for histological analysis. The esophagus was cut at the longitudinal axis and processed for the assessment of histological changes of squamous epithelium. The incidence and multiplicities of microscopic esophageal lesions were examined using histological sections of both macroscopically identified tumors and macroscopically normal-looking mucosa. All of the excised tissues, including the neoplastic nodules in the esophagus, were fixed for 24 h in neutral-buffered 10% formalin. The fixed samples were processed by standard methods, embedded in paraffin, sectioned at 5 μm, and stained with HE. The defining characteristics for dysplasia, papilloma, and SCC were adapted from previous reports in the literature.[16,17]

Immunostaining. The avidin–biotin–peroxidase complex (ABC) technique was used for immunohistochemical studies. Sections (5-μm thick) were cut, deparaffinized, rehydrated in PBS, placed in 10 mmol/L citrate buffer (pH 6.0), and heated in a 750-W microwave four times for 6 min. The endogenous peroxidase activity was blocked by incubation for 10 min in 0.3% H_2O_2. After washing three times with PBS, the sections were preincubated with normal blocking serum for 20 min at room temperature and then incubated with Ki-67 (1:200; DAKO, Glostrup, Denmark) and CK19 (1:500; Abcam, Cambridge, MA, USA) overnight at 4°C. Subsequently, the sections were incubated with biotinylated secondary antibodies (Vectastain ABC kit; Vector Laboratories, Burlingame, CA, USA) for 30 min followed by incubation with avidin-coupled peroxidase (Vector Laboratories) for 30 min. The sections were developed with 3,3′-diaminobenzidine (DAB) using the DAKO Liquid DAB Substrate-Chromogen System (DAKO) and then counterstained with hematoxylin. No specific staining was observed in the negative control slides prepared without primary antibody.

Results

Reduced DNA methylation levels suppressed the squamous tumorigenesis induced by 4NQO in both the tongue and esophagus. All mice with the exception of one *Dnmt1*$^{chip/c}$ mouse survived at the end of the 20-week 4NQO drinking, and there were no differences in the survival rate during 4NQO administrations between *Dnmt1*$^{chip/c}$ mice and *Dnmt1*$^{chip/+}$ mice ($n = 22$ and 23 respectively). There were no detectable differences in pathological alterations in the liver, kidney, lung, or heart between *Dnmt1*$^{chip/+}$ and *Dnmt1*$^{chip/c}$ mice with or without 4NQO administration. The mice without 4NQO exposure did not develop neoplasms in any organs examined, including the tongue and esophagus at the time of death.

Cohorts of *Dnmt1*$^{chip/+}$ or *Dnmt1*$^{chip/c}$ genotypes were aged to 25 weeks and analyzed for macroscopic tumors in both the tongue and esophagus. Macroscopically, nodular and polypoid tongue tumors were observed in the dorsum and tip of the tongue in mice with both genotypes that were exposed to 4NQO (Fig. 1a–c). The incidences and multiplicities of macroscopic

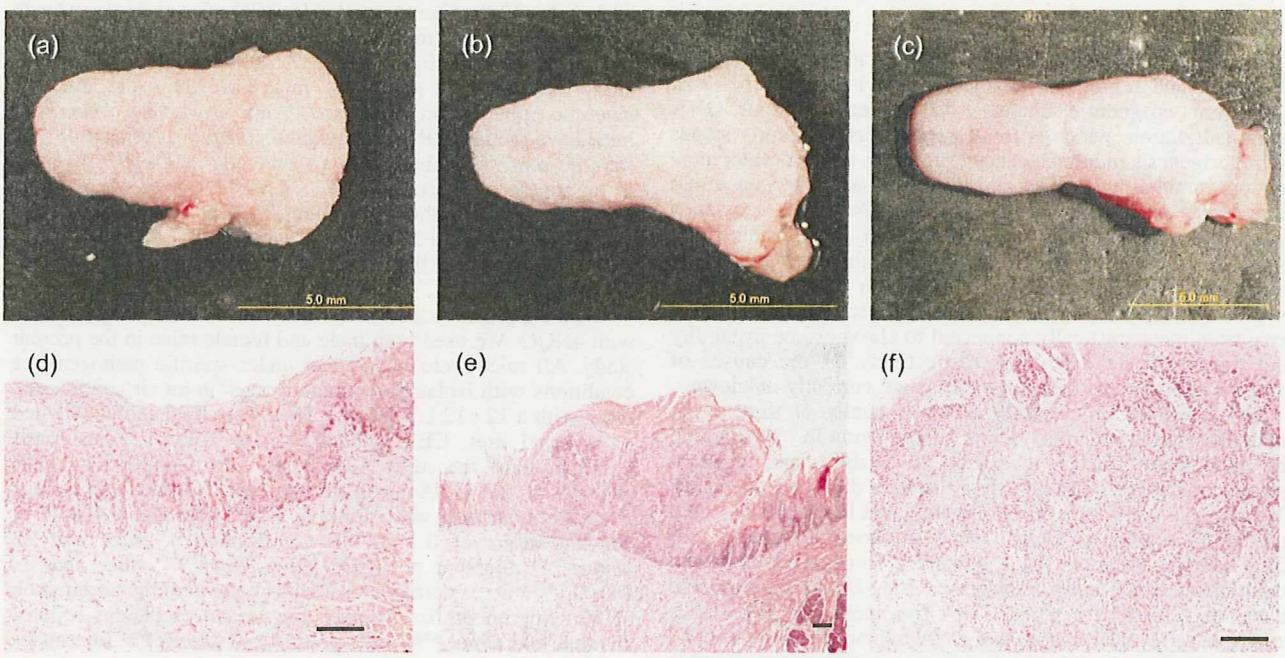

Fig. 1. Representative macroscopic appearance of the tongue and histology of different stages of squamous lesions. (a–c) Macroscopic appearance of the tongue. (a) 4-Nitroquinoline 1-oxide (4NQO)-exposed DNA methyltrasferase 1 (*Dnmt1*)$^{chip/+}$, (b) 4NQO-exposed *Dnmt1*$^{chip/c}$, and (c) the control *Dnmt1*$^{chip/+}$ mouse. Nodular and polypoid tumors are seen in the dorsum and tip of the tongue. (d–f) A histological sequence of epithelial changes from dysplasia through invasive squamous cell carcinoma. (d) Dysplasia, (e) papilloma, and (f) squamous cell carcinoma observed in the present study. Scale bars = 100 μm.

neoplasm in the tongue and esophagus are summarized in Table 1. In the present study, we did not observe any metastatic tumors. The incidence of macroscopic tongue tumors was 100 and 90.5% in *Dnmt1*$^{chip/+}$ and *Dnmt1*$^{chip/c}$ mice respectively. The multiplicity of macroscopic tongue tumors was 4.91 ± 1.02 and 1.90 ± 0.81 in *Dnmt1*$^{chip/+}$ and *Dnmt1*$^{chip/c}$ mice respectively. The multiplicity of macroscopic tongue tumors in *Dnmt1*$^{chip/c}$ mice was significantly smaller than *Dnmt1*$^{chip/+}$ mice (Table 1; $P < 0.05$). In the present study, we did not observe significant differences in the development of tumors between male and female mice. The size of macroscopic tumors in the tongue was significantly smaller in *Dnmt1*$^{chip/c}$ mice than *Dnmt1*$^{chip/+}$ mice (Table 1; $P < 0.005$). Next, we examined the development of microscopic lesions on the histological sections at the longitudinal center of the tongue. Histopathologically, dysplasia, papilloma, and SCC developed in the tongue of 4NQO-drinking mice of both genotypes (Fig. 1d–f). Histological assessment of squamous lesions at the longitudinal center of the tongue is summarized in Table 2. Although the development of early lesions of the tongue (dysplasia and papilloma) was not significantly different between *Dnmt1*$^{chip/c}$ and *Dnmt1*$^{chip/+}$ mice, both the incidence and multiplicity of SCC in *Dnmt1*$^{chip/c}$ mice were significantly lower than those in the control *Dnmt1*$^{chip/+}$ mice (Table 2; $P < 0.005$ and $P < 0.01$ respectively).

The incidence of macroscopic esophageal tumors was 78.3 and 42.9% with a multiplicity of 1.30 ± 1.04 and 0.62 ± 0.81 in *Dnmt1*$^{chip/+}$ and *Dnmt1*$^{chip/c}$ mice respectively (Table 1). Both the incidence and multiplicity of the macroscopic esophageal tumors were significantly smaller in *Dnmt1*$^{chip/c}$ mice than *Dnmt1*$^{chip/+}$ mice ($P < 0.05$). However, there was no significant difference in tumor size between two cohorts, with size of 1.82 ± 1.04 and 1.38 ± 0.68 mm in *Dnmt1*$^{chip/+}$ and *Dnmt1*$^{chip/c}$ mice respectively. Histological analyses revealed that both *Dnmt1*$^{chip/+}$ and *Dnmt1*$^{chip/c}$ mice with 4NQO administration developed dysplasia, squamous papilloma, and SCC in the esophagus (Table 2). Consistent with the results in the tongue, the incidence and multiplicity of microscopic SCC in the esophagus were significantly smaller in *Dnmt1*$^{chip/c}$ mice than in *Dnmt*$^{chip/+}$ mice (Table 2; $P < 0.01$ and $P < 0.05$ respectively), whereas those of papillomas were not different between the two cohorts.

Table 1. Incidences and multiplicities of macroscopic tumors of the tongue and esophagus

	Allele	Tongue	Esophagus
Incidence	chip/+	100.0	78.3
(%)	chip/c	90.5	42.9*
Multiplicity	chip/+	4.91 ± 1.02	1.30 ± 1.04
(mean ± SD)	chip/c	1.90 ± 0.81*	0.62 ± 0.81*
Diameter (mm)	chip/+	2.07 ± 0.57	1.82 ± 1.04
(mean ± SD)	chip/c	1.30 ± 0.67**	1.38 ± 0.68

*Significantly different from chip/+ ($P < 0.05$).
**Significantly different from chip/+ ($P < 0.005$).
chip/+, control mice; chip/c, hypomethylated mice.

DNA hypomethylation suppresses increased cell proliferation activity in the squamous epithelium exposed to 4NQO. In order to clarify the inhibitory mechanisms of the reduced DNA methylation levels on squamous tumorigenesis, we assessed the cell proliferation activity in non-tumoral squamous epithelium in the tongue by immunostaining for Ki-67, a marker for proliferating cells. 4NQO administration resulted in an increased ratio of Ki-67-positive cells in non-tumoral squamous epithelium of both *Dnmt1*$^{chip/+}$ and *Dnmt1*$^{chip/c}$ mice in comparison with non-treated mice (Fig. 2a). The results suggest that 4NQO induces abnormal cell proliferation even in the non-tumoral epithelium, which may support the concept of 'field cancerization'.[18,19] Importantly, the Ki-67-positive ratio was significantly lower in the tongue of *Dnmt1*$^{chip/c}$ mice in comparison with *Dnmt1*$^{chip/+}$ mice, indicating that reduced levels of genomic methylation suppress the cell proliferation activity that is activated by 4NQO administration (Fig. 2a). Additionally, the Ki-67-positive cell ratio in non-tumoral epithelium of the esophagus of 4NQO-exposed *Dnmt1*$^{chip/c}$ mice was significantly lower than that of 4NQO-exposed *Dnmt1*$^{chip/+}$ mice (Fig. 2b).

Expansion of CK19-positive progenitor cells by 4NQO was blocked in DNA hypomethylated mice. In order to examine the differentiation status of squamous epithelium, we carried out immunostaining for CK19, a marker of undifferentiated cells at the basal–suprabasal cell layer of squamous epithelium in the tongue.[20,21] Previous study revealed that the SCC contain an increased number of CK19-expressing cells in comparison with normal squamous epithelium,[21] suggesting that expansion of undifferentiated cells is involved in the tumorigenesis. Interestingly, non-tumoral mucosa exposed to 4NQO revealed a thickening of the CK19-positive layer in comparison with non-exposed tongue (Fig. 3a,b,d). An increased ratio of CK19-expressing layer to total epithelial thickness was also observed in 4NQO-exposed tongue (Fig. 3e). The results suggest that 4NQO exposure increases the number of CK19-expressing progenitor cells and inhibits the cellular differentiation of squamous epithelium. Importantly, the expansion of squamous progenitors by the administration of 4NQO was blocked in DNA hypomethylated mice (Fig. 3c–e), thus indicating that DNA methylation plays a role in the suppression of cellular differentiation in the tongue.

Table 2. Incidences and multiplicities of microscopic tumors of the tongue and esophagus

	Allele	Tongue†			Esophagus		
		Dysplasia	Papilloma	SCC	Dysplasia	Papilloma	SCC
Incidence	chip/+	91.3	17.4	60.9	100.0	13.0	82.6
(%)	chip/c	81.0	4.8	19.0*	71.4**	19.0	42.9**
Multiplicity	chip/+	1.61 ± 0.99	0.17 ± 0.39	0.91 ± 0.85	2.26 ± 1.66	0.14 ± 0.34	1.30 ± 1.22
(Mean ± SD)	chip/c	1.52 ± 1.21	0.05 ± 0.22	0.19 ± 0.40**	1.48 ± 1.47	0.19 ± 0.40	0.48 ± 0.60***

*Significantly different from chip/+ ($P < 0.005$).
**Significantly different from chip/+ ($P < 0.01$).
***Significantly different from chip/+ ($P < 0.05$).
†Incidences and multiplicities of microscopic tumors in the tongue were determined on the histological sections at the longitudinal center of the tongue.
chip/+, control mice; chip/c, hypomethylated mice.

doi: 10.1111/j.1349-7006.2009.01171.x

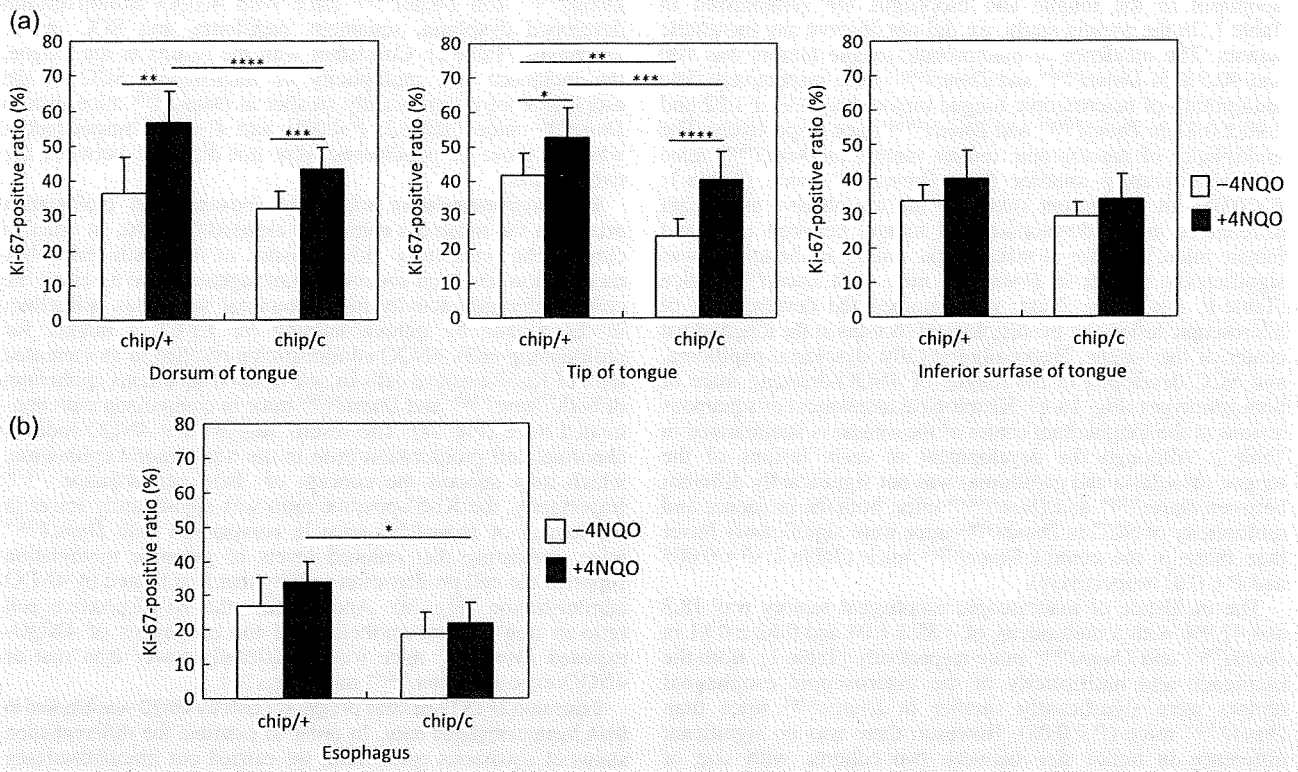

Fig. 2. Percentage of Ki-67-positive cells in non-tumoral squamous epithelium of both DNA methyltrasferase 1 (*Dnmt1*)$^{chip/+}$ and *Dnmt1*$^{chip/c}$ mice. (a) The Ki-67-positive ratio at the non-tumoral squamous epithelium of the tongue. 4-Nitroquinoline 1-oxide (4NQO) administration resulted in an increased ratio of Ki-67-positive cells in squamous epithelium at the dorsum and tip of the tongue where direct exposure of 4NQO is expected. In contrast, the ratio at the inferior surface where 4NQO exposure is expected to be less than other sites did not change. The Ki-67-positive ratio is significantly lower in *Dnmt1*$^{chip/c}$ mice in comparison with *Dnmt1*$^{chip/+}$ mice, suggesting that DNA hypomethylation suppresses cell proliferative activity. $*P < 0.05$, $**P < 0.01$, $***P < 0.005$, $****P < 0.001$. (b) The Ki-67-positive ratio at the non-tumoral squamous epithelium of the esophagus. The Ki-67-positive ratio in *Dnmt1*$^{chip/c}$ mice exposed to 4NQO is significantly lower than that in *Dnmt1*$^{chip/+}$ mice exposed to 4NQO. $*P < 0.001$.

Discussion

Here we have shown that genetic reduction of DNA methylation levels suppresses squamous tumorigenesis in both tongue and esophagus. The findings that genomic hypomethylation significantly inhibited SCC development in both tongue and esophagus suggest that DNA methylation plays a role in the progression stage of the squamous carcinogenesis in the upper digestive tract.

Expansion of stem and progenitor cells is a driving force in tumorigenesis.[22] Consistent with the notion, many tumors express genes that are expressed in the undifferentiated cells of the target organs.[22] In the present study, we showed that 4NQO exposure increases the number of CK19-expressing progenitor cells[20,21] and that global DNA hypomethylation suppresses such expansion of progenitor cells in the tongue. Given the fact that squamous progenitors proliferate actively, these findings suggest that the suppression of cellular differentiation, which is associated with DNA methylation, causes the expansion of proliferating progenitor cells, eventually leading to tumorigenesis in the tongue. The hypothesis is also consistent with our findings that the Ki-67-positive cell ratio is suppressed in the tongue of DNA hypomethylated mice. In the present study, suppression of the Ki-67-positive ratio by DNA hypomethylation was also observed in the esophagus. Recently, mouse esophageal stem cells have been identified using a label-retaining method. It would be of interest to examine the effect of the genomic DNA hypomethylation on the number of stem and progenitor cells in the esophageal tumors.

It is also noteworthy that a previous study indicated that expansion of undifferentiated cells is directly associated with invasive growth of epithelial cells.[22] Our findings that DNA hypomethylation promotes cellular differentiation and suppresses the development of invasive tumors may provide an additional link between the maintenance of undifferentiated states and the invasive growth of cancer cells. The observation that abnormal DNA methylation is associated with the maintenance of undifferentiated states is also consistent with previous findings, in which targets of abnormal DNA methylation in cancer cells are shown to be frequently overlapping with targets of the polycomb complex that is important to suppress cellular differentiation by silencing differentiation-associated genes in embryonic stem (ES) cells.[23,24] It is possible that the genes that are involved in cellular differentiation of the squamous epithelium are the targets of site-specific DNA hypermethylation in 4NQO-induced carcinogenesis.

Target genes of the abnormal DNA methylation in squamous lesions of this mouse model are not yet clear. Although it has been reported that the promoter regions of *p16Ink4a* and *p15Ink4b* are methylated in 4NQO-induced rat tongue cancers,[25] we failed to detect DNA hypermethylation at *p16Ink4a* by methylation-specific PCR in the present study (data not shown). Understanding the epigenetic controls in the cellular

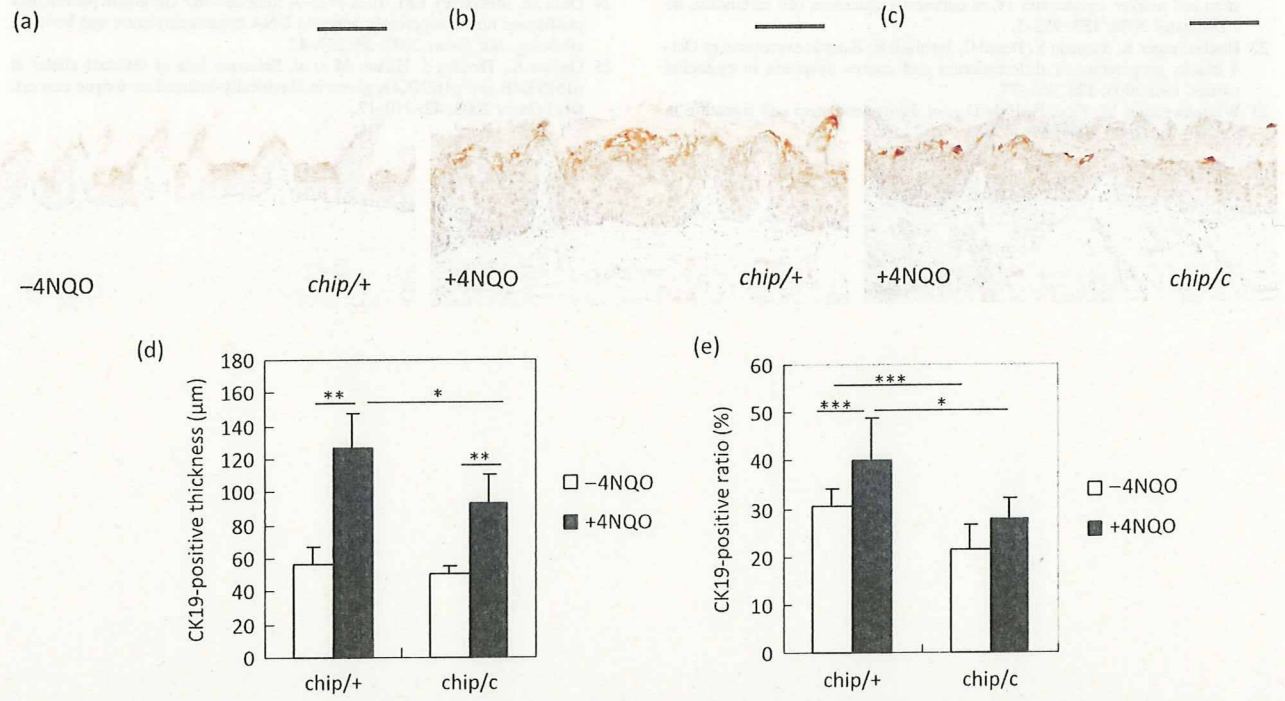

Fig. 3. Expansion of the CK19-positive cell layer in 4-nitroquinoline 1-oxide (4NQO)-exposed tongue epithelium and its suppression by genomic hypomethylation. (a–c) CK19 immunohistological staining of tongue squamous epithelium. (a) 4NQO non-exposed DNA methyltrasferase 1 (*Dnmt1*)$^{chip/+}$ mice. (b) 4NQO exposed *Dnmt1*$^{chip/+}$ mice. (c) 4NQO exposed *Dnmt1*$^{chip/c}$ mice. Note that 4NQO exposure resulted in increased thickness of the CK19-positive layer, whereas such an effect was less prominent in DNA hypomethylated mice. Scale bars = 100 μm. (d) Thickness of CK19-positive cells (μm). (e) The CK19-positive ratio at the dorsum of the tongue. *$P < 0.001$, **$P < 0.005$, ***$P < 0.05$.

differentiation of normal squamous epithelium might uncover the mechanisms underlying DNA methylation-associated tumorigenesis in the tongue and esophagus. Further analyses are required to identify genes that connect the abnormal genomic hypermethylation and altered differentiating potential involved in cancer cells.

Acknowledgment

We thank Kyoko Takahashi, Ayako Suga, and Yoshitaka Kinjyo for the technical assistance and animal care. This study was supported by grants from the Ministry of Health, Labour, and Welfare of Japan, and grants from the Ministry of Education, Culture, Sports, Science, and Technology of Japan.

References

1 Jones PA, Baylin SB. The fundamental role of epigenetic events in cancer. *Nat Rev Genet* 2002; **3**: 415–28.
2 Chen RZ, Pettersson U, Beard C, Jackson-Grusby L, Jaenisch R. DNA hypomethylation leads to elevated mutation rates. *Nature* 1998; **395**: 89–93.
3 Toyota M, Ahuja N, Ohe-Toyota M, Herman JG, Baylin SB, Issa JP. CpG island methylator phenotype in colorectal cancer. *Proc Natl Acad Sci USA* 1999; **96**: 8681–6.
4 Yamada Y, Jackson-Grusby L, Linhart H *et al.* Opposing effects of DNA hypomethylation on intestinal and liver carcinogenesis. *Proc Natl Acad Sci USA* 2005; **102**: 13 580–5.
5 Laird PW, Jackson-Grusby L, Fazeli A *et al.* Suppression of intestinal neoplasia by DNA hypomethylation. *Cell* 1995; **81**: 197–205.
6 Li E, Bestor TH, Jaenisch R. Targeted mutation of the DNA methyltransferase gene results in embryonic lethality. *Cell* 1992; **69**: 915–26.
7 Okano M, Bell DW, Haber DA, Li E. DNA methyltransferases Dnmt3a and Dnmt3b are essential for de novo methylation and mammalian development. *Cell* 1999; **99**: 247–57.
8 Linhart HG, Lin H, Yamada Y *et al.* Dnmt3b promotes tumorigenesis *in vivo* by gene-specific de novo methylation and transcriptional silencing. *Genes Dev* 2007; **21**: 3110–22.
9 Gaudet F, Hodgson JG, Eden A *et al.* Induction of tumors in mice by genomic hypomethylation. *Science* 2003; **300**: 489–92.
10 Eden A, Gaudet F, Waghmare A, Jaenisch R. Chromosomal instability and tumors promoted by DNA hypomethylation. *Science* 2003; **300**: 455.
11 Nakahara W, Fukuoka F, Sugimura T. Carcinogenic action of 4-nitroquinoline-*N*-oxide. *Gan* 1957; **48**: 129–37.
12 Ikenaga M, Ishii Y, Tada M, Kakunaga T, Takebe H. Excision-repair of 4-nitroquinolin-1-oxide damage responsible for killing, mutation, and cancer. *Basic Life Sci* 1975; **5B**: 763–71.
13 Tang XH, Knudsen B, Bemis D, Tickoo S, Gudas LJ. Oral cavity and esophageal carcinogenesis modeled in carcinogen-treated mice. *Clin Cancer Res* 2004; **10**: 301–13.
14 Tanaka T, Makita H, Ohnishi M *et al.* Chemoprevention of 4-nitroquinoline 1-oxide-induced oral carcinogenesis in rats by flavonoids diosmin and hesperidin, each alone and in combination. *Cancer Res* 1997; **57**: 246–52.
15 Lei H, Oh SP, Okano M *et al.* De novo DNA cytosine methyltransferase activities in mouse embryonic stem cells. *Development* 1996; **122**: 3195–205.
16 Gunji A, Uemura A, Tsutsumi M *et al.* Parp-1 deficiency does not increase the frequency of tumors in the oral cavity and esophagus of ICR/129Sv mice by 4-nitroquinoline 1-oxide, a carcinogen producing bulky adducts. *Cancer Lett* 2006; **241**: 87–92.
17 Ide F, Oda H, Nakatsuru Y *et al.* Xeroderma pigmentosum group A gene action as a protection factor against 4-nitroquinoline 1-oxide-induced tongue carcinogenesis. *Carcinogenesis* 2001; **22**: 567–72.
18 Slaughter DP, Southwick HW, Smejkal W. Field cancerization in oral stratified squamous epithelium; clinical implications of multicentric origin. *Cancer* 1953; **6**: 963–8.
19 Ushijima T. Epigenetic field for cancerization. *J Biochem Mol Biol* 2007; **40**: 142–50.
20 Lindberg K, Rheinwald JG. Suprabasal 40 kd keratin (K19) expression as an immunohistologic marker of premalignancy in oral epithelium. *Am J Pathol* 1989; **134**: 89–98.
21 Chen S, Takahara M, Kido M *et al.* Increased expression of an epidermal

doi: 10.1111/j.1349-7006.2009.01171.x

stem cell marker, cytokeratin 19, in cutaneous squamous cell carcinoma. *Br J Dermatol* 2008; **159**: 952–5.
22 Hochedlinger K, Yamada Y, Beard C, Jaenisch R. Ectopic expression of Oct-4 blocks progenitor-cell differentiation and causes dysplasia in epithelial tissues. *Cell* 2005; **121**: 465–77.
23 Widschwendter M, Fiegl H, Egle D *et al.* Epigenetic stem cell signature in cancer. *Nat Genet* 2007; **39**: 157–8.
24 Ohm JE, McGarvey KM, Yu X *et al.* A stem cell-like chromatin pattern may predispose tumor suppressor genes to DNA hypermethylation and heritable silencing. *Nat Genet* 2007; **39**: 237–42.
25 Ogawa K, Tanuma J, Hirano M *et al.* Selective loss of resistant alleles at p15INK4B and p16INK4A genes in chemically-induced rat tongue cancers. *Oral Oncol* 2006; **42**: 710–17.

Laboratory/Clinical Translational Research

Oncology

Oncology 2008;74:50–60
DOI: 10.1159/000139124

Received: November 16, 2007
Accepted after revision: January 17, 2008
Published online: June 11, 2008

Identification of Genes Targeted by CpG Island Methylator Phenotype in Neuroblastomas, and Their Possible Integrative Involvement in Poor Prognosis

Masanobu Abe[a, b] Naoko Watanabe[a] Nathalie McDonell[a] Tsuyoshi Takato[b]
Miki Ohira[c] Akira Nakagawara[c] Toshikazu Ushijima[a]

[a]Carcinogenesis Division, National Cancer Center Research Institute, [b]Department of Oral and Maxillofacial Surgery, University of Tokyo Graduate School of Medicine and [c]Biochemistry Division, Chiba Cancer Center Research Institute, Tokyo, Japan

Key Words
Neuroblastoma · Methylation · Silencing · CpG island methylator phenotype · Prognosis

Abstract
Background/Aims: CpG island (CGI) methylator phenotype (CIMP) is strongly associated with poor prognosis in neuroblastomas (NBLs; hazard ratios 7–22). Methylation of nonpromoter CGIs is useful to detect the presence of the CIMP, while the poor prognosis is considered to be caused by gene silencing due to promoter methylation. Here, promoter CGIs targeted by the CIMP were searched for. ***Methods:*** A genome-wide screening was performed by methylation-sensitive representational difference analysis of CIMP(+) and CIMP(–) NBLs. ***Results:*** Promoter CGIs of 9 genes were methylated in CIMP(+) NBL cell lines and caused silencing of their downstream genes. On analysis of 90 clinical specimens, *CYP26C1*, *FERD3L* (*N-TWIST*), *CRYBA2* and *PCDHGC4* were methylated at significantly higher incidences in CIMP(+) NBLs than CIMP(–) NBLs, while the difference was unclear for *NPY*, *SPAG6*, *DDIT4L*, *CHR3SYT* and *C6Orf141*. Methylation of *CYP26C1* and *FERD3L* was significantly associated with poor prognosis, but weaker than the presence of the CIMP. Treatment of an NBL cell line with a demethylating agent caused demethylation of multiple promoter CGIs, and enhanced 13-*cis*-retinoic acid-induced neuronal differentiation. ***Conclusion:*** Our results indicate that the CIMP causes poor prognosis of NBLs by inducing methylation of multiple promoter CGIs with various incidences.

Introduction

The CpG island (CGI) methylator phenotype (CIMP), characterized by methylation of multiple CGIs, was first identified in colorectal cancers [1], and has been detected in various tumors [2]. In neuroblastomas (NBLs), the most common extracranial pediatric solid tumors [3], the CIMP was found to be associated with poor survival with extremely high hazard ratios (HR), reaching as high as 22 [95% confidence interval (CI) 5.3–93] and 9.5 (95% CI = 3.2–28) in Japanese and German cases, respectively [4, 5]. Strikingly, the NBL cases with the CIMP included almost all cases with N-*myc* amplification (37/38 Japanese and 23/23 German cases), the strongest current prognostic marker [6–8]. Even among the cases without N-*myc* amplification, the CIMP was a significant and strong prognostic marker [4, 5].

KARGER
Fax +41 61 306 12 34
E-Mail karger@karger.ch
www.karger.com

0030–2414/08/0742–0050$24.50/0

Accessible online at:
www.karger.com/ocl

Toshikazu Ushijima
5-1-1 Tsukiji, Chuo-ku
Tokyo 104-0045 (Japan)
Tel. +81 3 3547 5240, Fax +81 3 5565 1753, E-Mail tushijim@ncc.go.jp

In individual tumor types, the CIMP has been analyzed using CGIs specific to them [2]. In NBLs, the CIMP is most sensitively detected by methylation of nonpromoter CGIs of (1) the *PCDH-β* gene family, (2) the *PCDH-α* gene family, (3) *HLP* and its pseudogene and (4) *CYP26C1* [4]. Generally, CGIs in nonpromoter regions are susceptible to de novo methylation, and their methylation does not repress transcription [9, 10]. As expected, methylation of the 4 nonpromoter CGIs in NBLs did not, and was unlikely to be involved in the poor prognosis directly. However, their methylation was associated with methylation of promoter CGIs of tumor suppressor genes, such as *RASSF1A* and *BLU*, with low incidences [4]. Also, it is reported that methylation of the *HOXA9* and *EMP3* promoter CGIs is associated with poor prognosis, with hazard ratios smaller than those given by the CIMP [11, 12]. This suggested that the CIMP invariably induces methylation of susceptible CGIs (specific nonpromoter CGIs) and occasionally induces methylation of resistant CGIs (promoter CGIs). The latter can cause gene silencing and be involved in the poor prognosis of NBL cases.

However, only a limited number of promoter CGIs targeted by the CIMP in NBLs have been identified so far. Here, we aimed to identify such promoter CGIs, and performed a genome-wide screening procedure for differences in DNA methylation, methylation-sensitive representational difference analysis (MS-RDA) [13–15]. Since promoter CGIs of genes involved in neuronal development and differentiation were identified, we also analyzed the effect of a demethylating agent, 5-aza-2′-deoxycytidine (5-aza-dC), on differentiation induction of NBL cell lines by 13-*cis*-retinoic acid (13-*cis*-RA), which is now recognized to be effective even in NBL cases with high risk [16].

Materials and Methods

Tissue Samples and Cell Lines

Tumor samples were obtained from 90 nonrecurrent Japanese cases between 1995 and 1999, and were analyzed under the approval of institutional review boards. The mean age at initial diagnosis was 29 months (range 0–216). Their clinical stages were determined according to the International Neuroblastoma Staging System: 32 (2, excluding cases identified by mass screening and cases without data on prognosis), 13 (2), 7 (5), 30 (29) and 8 (5) cases belonging to stages 1, 2, 3, 4 and 4S, respectively. Normal adrenal medulla tissue was collected from a case undergoing nephrectomy due to a renal cancer. NBL cell lines and a neuroepithelioma cell line were obtained from the American Type Culture Collection (Manassas, Va., USA), the Japanese Collection of Research Bioresources (Tokyo, Japan), the Cell Resource Center for Biomedical Research, Institute of Development, Aging and Cancer, Tohoku University (Sendai, Japan) and the RIKEN Bio Resource Center (Tsukuba, Japan). High molecular weight DNA and total RNA were extracted as previously described [17].

Detection of the CIMP

NBLs with the CIMP were defined as in our previous reports [4, 5]. The methylation level, the fraction of methylated DNA molecules among the total DNA molecules, of the *PCDH-β* gene family was quantitatively determined by quantitative methylation-specific PCR (MSP), and cases with methylation levels higher than 40% were diagnosed as those with the CIMP.

MS-RDA and Database Search

MS-RDA was performed as previously described [13–15]. To isolate DNA fragments specifically methylated in CIMP(+) NBLs, 4 series of MS-RDA were performed using a CIMP(–) NBL as the tester and a CIMP(+) NBL cell line as the driver. In 2 series, IMR-32 cell line (methylation level of the *PCDH-β* gene family: 99%) was commonly used as the driver, and case 188 (13%) or 216 (23%) as the tester. In the other 2 series, TGW cell line (99%) was commonly used as the driver, and case 212 (19%) or 215 (20%) as the tester. The tester and driver samples were digested with a methylation-sensitive restriction enzyme, *Hpa*II (New England Biolabs, Beverly, Mass., USA), and the restriction product was amplified using a universal adaptor and primer in the presence of 1 M betaine (Sigma, St. Louis, Mo., USA). DNA fragments present only in the tester PCR product were amplified by the following genomic subtraction technique, RDA [18]. Although use of cell lines is highly recommended for MS-RDA [13], no cell lines were available for NBLs with a good prognosis, and therefore we used the primary samples [4]. One hundred clones were sequenced for each series of MS-RDA (total 400 clones), and nonredundant clones were selected. The genomic origins of the nonredundant clones were searched for using BLASTN software (http://www.ncbi.nlm.nih.gov/BLAST/). CGIs were searched for using CpG Island Searcher (http://cpgislands.usc.edu/) [19].

Sodium Bisulfite Modification and MSP

Five hundred nanograms of DNA underwent sodium bisulfite modification [20], and was suspended in 20 μl of TE buffer. For MSP [21], 1 μl of the solution was used as a template for PCR with primers specific to methylated or unmethylated sequences. As universally methylated and unmethylated DNA, genomic DNA methylated with *Sss*I methylase (New England Biolabs) and DNA amplified with phi29 DNA polymerase (GE Healthcare, Uppsala, Sweden) [22] were used, respectively. Specific annealing temperatures for methylated and unmethylated primers were determined, and a number of PCR cycles for more than the minimal numbers was adopted. The methylation status of the *CYP26C1* promoter region was determined by quantitative MSP as previously described [5], and a cutoff value of 60% was adopted. The primers and PCR conditions are shown in online supplement table 1 (www.karger.com/doi/10.1159/000139124).

Quantitative RT-PCR

cDNA was synthesized from 3 μg of total RNA treated with DNase I using a SuperScript II kit (Invitrogen, Carlsbad, Calif., USA). The numbers of cDNA molecules were determined by comparing their amplification curves with those of standard samples with known numbers of template DNA molecules by real-time

Table 1. Methylation of the 8 genes identified by MS-RDA and CYP26C1

Gene			Fragment obtained by MS-RDA			Methylation in clinical specimens			Overall survival		
symbol	name	chromosome	accession No.	from	to	CIMP (–)	CIMP (+)	p value	HR	95% CI	p value
CYP26C1	cytochrome P450, subfamily 26C1	10q23	NA	NA	NA	0/54	27/36	<0.001	12.3 (3.0)	4.1–36.9 (1.0–8.9)	<0.001 (0.05)
FERD3L (N-TWIST)	Fer3-like *(Drosophila)*	7p21	AC003986	107,728	108,128	2/54	20/36	<0.001	7.2 (2.6)	2.9–18.2 (1.0–6.6)	<0.001 (0.04)
CRYBA2	crystallin, βA2	2q34	AC097468	73,363	73,635	4/54	13/35	<0.001	1.9 (1.4)	0.7–4.8 (0.6–3.8)	0.21 (0.46)
PCDHGC4	protocadherin-γ subfamily C, 4	5q31	NG000012	195,471	196,054	2/54	9/36	<0.01	2.3 (0.8)	0.8–6.8 (0.3–2.5)	0.14 (0.73)
NPY	neuropeptide Y	7p15	AC004485	155,699	156,102	1/54	2/36	0.34	NA	NA	NA
SPAG6	sperm-associated antigen 6	10p12	AL158211	100,932	101,345	1/49	1/33	0.78	NA	NA	NA
DDIT4L	DNA damage-inducible transcript 4-like	4q24	AP001961	21,100	21,259	0/54	1/36	0.22	NA	NA	NA
CHR3SYT	chr3 synaptotagmin	3q22	AC022497	86,544	86,887	0/53	0/33	NA	NA	NA	NA
C6orf141	chromosome 6 open reading frame 141	6p12	AL590244	72,303	72,802	0/54	0/36	NA	NA	NA	NA
CIMP	methylation of PCDH-β gene family	5q31	NA	NA	NA	54 (13)	36 (30)	NA	34.9 (10.9)	4.7–261 (1.5–81.5)	<0.001 (0.02)

Figures in parentheses are results in 43 cases after excluding 45 mass screening cases. NA = Not applicable.

PCR using SYBR Green Real-Time PCR Master Mix (Toyobo, Osaka, Japan) and the 7300 Real-Time PCR System (Applied Biosystems, Foster City, Calif., USA). The copy number was normalized to that of glyceraldehyde-3-phosphate dehydrogenase *(GAPDH)*. The primers and PCR conditions are shown in online supplement table 2 (www.karger.com/doi/10.1159/000139124).

*Treatment of Cells by 5-aza-dC and 13-*cis*-RA*

5-Aza-dC (Sigma) was dissolved in PBS and diluted in cell culture medium to obtain final concentrations as specified. 13-*cis*-RA (Sigma) was dissolved in dimethylsulfoxide and diluted in cell culture medium to obtain final concentrations of 1 μM. All experiments using 13-*cis*-RA were performed in dim light, and the final concentration of dimethylsulfoxide was 0.001%.

For demethylation and re-expression analysis, cells were seeded on day 0 at a density of 1×10^5 cells/10-cm dish and exposed to 0, 1, 3 and 10 μM 5-aza-dC for 24 h on days 1, 3, 5 and 7, and harvested on day 8. For cell growth and differentiation analyses, cells were seeded on day 0 at a density of 3×10^4 cells/6-cm dish in triplicate, and the number of cells was counted on days 1, 2, 3, 4 and 5. The experiments were repeated twice. The possible presence of apoptotic cells was evaluated by detecting nicked DNA, using a DeadEnd™ fluorometric TUNEL system kit (Promega, Tokyo, Japan). NB-39nu cells treated with DNase I were used as a positive control.

Statistical Analysis

Survival time in NBL cases was measured from the date of initial diagnosis to the date of death or last contact. Kaplan-Meier analysis and log-rank tests were performed to compare overall survival between 2 groups. HR was estimated by the Cox proportional hazards model. These statistical analyses were performed using Dr. SPSS II, version 11.0 (SPSS Inc., Chicago, Ill., USA).

Results

Genome-Wide Screening for Promoter CGIs Methylated in CIMP(+) NBLs

To isolate DNA fragments specifically methylated in CIMP(+) NBLs, 4 series of MS-RDA were performed using a CIMP(–) NBL as the tester and a CIMP(+) NBL cell line as the driver. In 2 series, IMR-32 cell line (methylation level of the *PCDH-β* gene family: 99%) was commonly used as the driver, and case 188 (13%) or 216 (23%) as the tester. In the other 2 series, TGW cell line (99%) was commonly used as the driver, and case 212 (19%) or 215 (20%) as the tester. By the 4 series of MS-RDA, 181

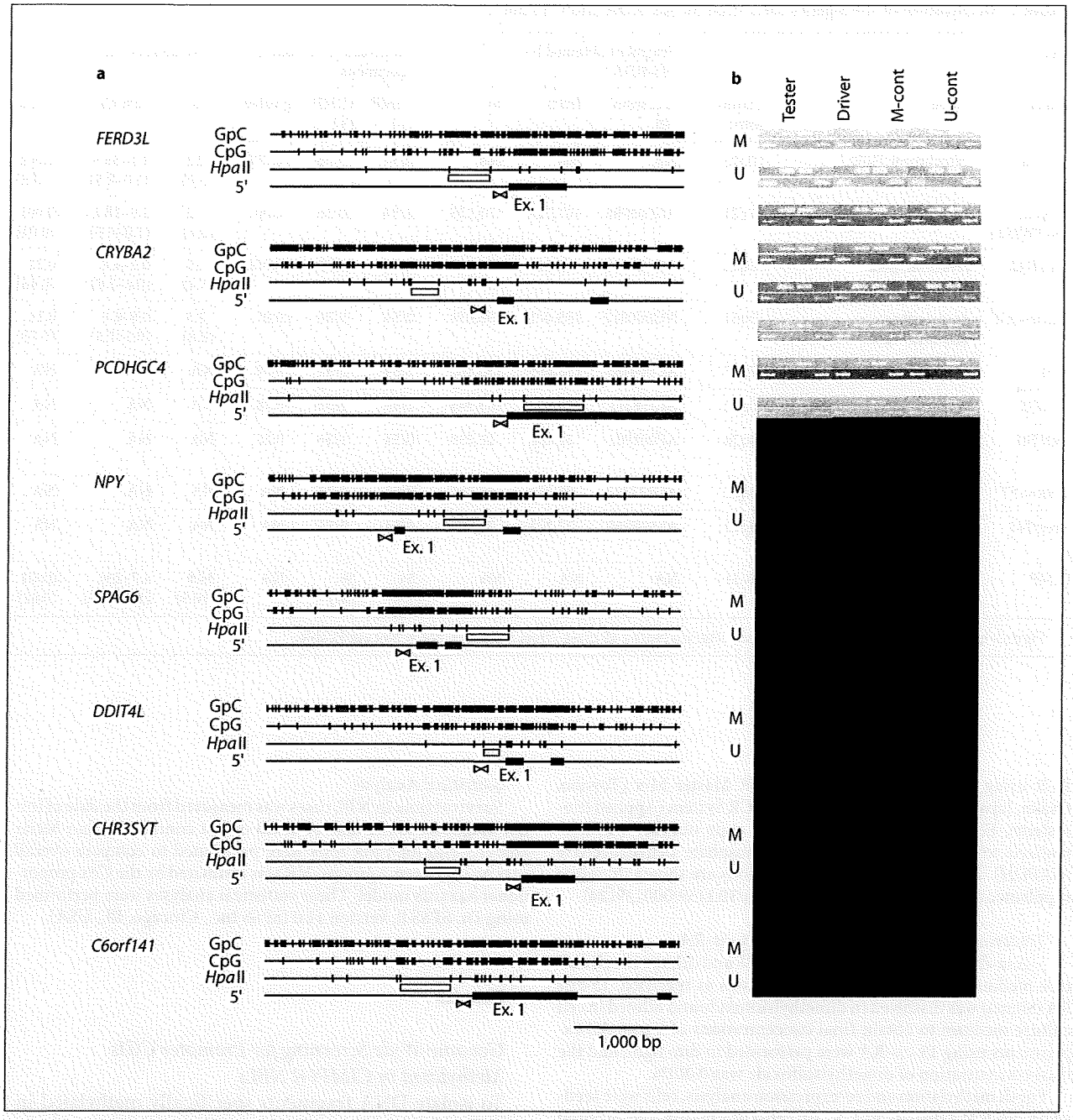

Fig. 1. Eight promoter CGIs isolated by MS-RDA and their methylation statuses in the samples used for MS-RDA. **a** Genomic structures of the 8 CGIs. GpC, CpG and *Hpa*II recognition sites (5′-CCGG-3′) are shown by ticks. Closed boxes = Exons; open boxes = clones isolated by MS-RDA; triangles = primers for MSP. **b** Methylation statuses analyzed by MSP. M = Primers specific to methylated DNA; U = primers specific to unmethylated DNA; M-cont = fully methylated DNA; U-cont = fully unmethylated DNA. All 8 CGIs were found to be differentially methylated between the 2 samples used for MS-RDA.

nonredundant DNA fragments were isolated, and 13 of them were derived from CGIs according the criteria set by Takai and Jones [19] in putative promoter regions.

Methylation of the 13 putative promoter CGIs was analyzed by MSP in the tester and driver DNA was used for the MS-RDA. Of the 13 CGIs, 8 genes [*FERD3L* (also known as *N-TWIST*, 7p21), *CRYBA2* (2q34), *PCDHGC4* (5q31), *NPY* (7p15), *SPAG6* (10p12), *DDIT4L* (4q24), *CHR3SYT* (3q22) and *C6orf141* (6p12)] were methylated in driver DNA and unmethylated tester DNA (fig. 1; table 1). *NPY*, *DDIT4L* and *C6orf141* were repeatedly isolated in 2, 4 and 2 series of MS-RDA, respectively.

Methylation of Promoter CGIs in Cell Lines

Methylation of the 8 genes mentioned above was further analyzed in 10 NBL cell lines, including IMR-32 and TGW, and a neuroepithelioma cell line, SK-N-MC (fig. 2). At the same time, methylation of a promoter CGI of *CYP26C1*, whose nonpromoter CGI was found to be methylated in our previous study [4], was analyzed. Representatively, a promoter CGI of *NPY* was completely methylated (no unmethylated DNA molecules detected) in 6 cell lines, partially methylated (both methylated and unmethylated DNA molecules detected) in 2 and completely unmethylated (no methylated DNA molecules detected) in 3 (fig. 2a). The 9 CGIs were methylated in 7–11 of the 11 cell lines (fig. 2b).

Methylation-Silencing of the 9 CGIs

Expression levels of the 9 genes mentioned above were analyzed by quantitative RT-PCR in the 11 cell lines and the primary adrenal medulla (fig. 3). For all genes, NBL cell lines with complete methylation of a gene did not express the gene (<1/900 of expressing cells). Five genes, *CYP26C1*, *CRYBA2*, *NPY*, *DDIT4L* and *CHR3SYT*, were expressed in the adrenal medulla, while the remaining 4, *FERD3L*, *PCDHGC4*, *SPAG6* and *C6orf141*, were not.

To analyze whether the expression loss of these 9 genes was really due to methylation of their promoter CGIs, 2 NBL cell lines, IMR-32 and TGW, were treated with a demethylating agent, 5-aza-dC (data for IMR-32 shown in fig. 4; data for TGW not shown). Demethylation of the promoter CGIs and restoration of their expression were observed for all 9 genes, showing that these genes were silenced by methylation of their promoter CGIs.

Association between the CIMP and Promoter Methylation in Clinical Specimens

To examine the association between the presence of the CIMP and methylation of the promoter CGIs in NBL clinical specimens, methylation of the 9 genes was analyzed in 90 clinical specimens whose CIMP statuses were determined by quantitative MSP of the *PCDH-β* gene family in our previous study (representative results shown in fig. 5a, summarized in fig. 5b and table 1) [4]. It was shown that *CYP26C1*, *FERD3L*, *CRYBA2* and *PCDHGC4* were methylated at significantly higher incidences in CIMP(+) NBL cases ($p < 0.001$ or 0.01). *NPY*, *SPAG6* and *DDIT4L* were also methylated with low incidences in CIMP(+) NBL cases, while *CHR3SYT* and *C6orf141* were not methylated in either group. This showed that promoter CGIs of *CYP26C1*, *FERD3L*, *CRYBA2* and *PCDHGC4* are targets of the CIMP, while those of *NPY*, *SPAG6* and *DDIT4L* are possible targets.

The association between the methylation of the 9 promoter CGIs and prognosis was further analyzed. Data on the overall survival were available for 88 (43 non-mass screening cases) of the 90 cases (table 1). The numbers of

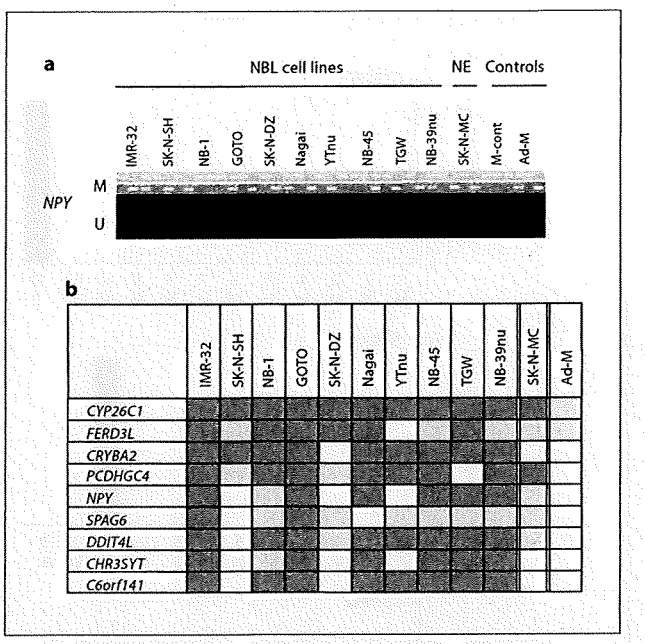

Fig. 2. Methylation analysis of the 9 promoter CGIs in 10 NBL cell lines and a neuroepithelioma cell line (NE), SK-N-MC, by MSP. **a** Representative result of MSP *(NPY)* of the 11 cell lines, fully methylated DNA (M-cont) and the normal adrenal medulla (Ad-M). M = Primers specific to methylated DNA; U = primers specific to unmethylated DNA. **b** Methylation profile of the 9 promoter CGIs in the 11 cell lines and the normal adrenal medulla (Ad-M). Closed boxes = Only methylated DNA detected; gray boxes = both methylated and unmethylated DNA detected; open boxes = only unmethylated DNA detected.

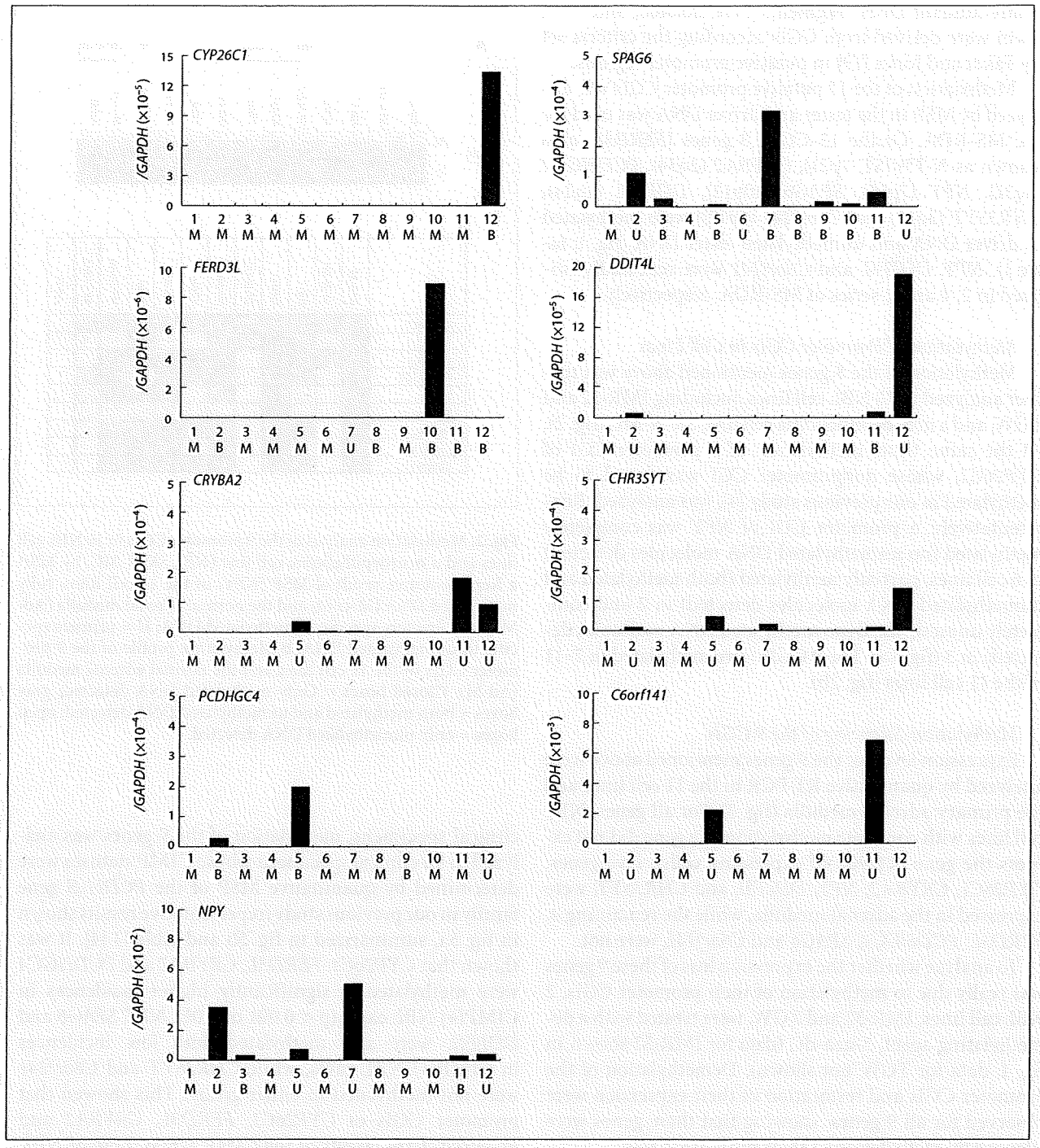

Fig. 3. Expression levels of the 9 genes in the 11 cell lines and the normal adrenal medulla by quantitative RT-PCR. Samples No. 1–10 are NBL cell lines (IMR-32, SK-N-SH, NB-1, GOTO, SK-N-DZ, Nagai, YTnu, NB-45, TGW and NB-39nu, respectively), sample No. 11 is neuroepithelioma cell line (SK-N-MC) and sample No. 12 is normal adrenal medulla tissue. Results of MSP are summarized under the sample numbers. The expression levels of these 9 genes in cell lines with only methylated DNA were extremely low or null. M = Only methylated DNA detected; B = both methylated and unmethylated DNA detected; U = only unmethylated DNA detected.

CIMP(–) and CIMP(+) cases were 52 (13) and 36 (30), respectively. Methylation of 2 promoter CGIs (*CYP26C1* and *FERD3L*) was significantly associated with overall survival with HRs of 12.3 (95% CI 4.1–36.9; $p < 0.001$) and 7.2 (2.9–18.2, $p < 0.001$), as well as 3.0 (1.0–8.9, $p = 0.05$) and 2.6 (1.0–6.6, $p = 0.04$) for non-mass screening cases, respectively. The HRs given by these 2 genes were smaller than the HR given by the CIMP (methylation of the *PCDH-β* family; 34.9, 4.7–261.0, $p < 0.001$ for all cases; 10.9, 1.5–81.5, $p = 0.02$ for non-mass screening cases), but their methylation was considered to underlie the poor prognosis of the CIMP(+) cases by causing gene silencing.

Effect of a Demethylating Agent on Differentiation of NBL Cell Lines

Among the target genes of the CIMP, there was a regulator of neurogenesis, *FERD3L* [23], and a neuronal differentiation marker, *NPY* [24]. This suggested that reactivation of these target genes by a demethylating agent could enhance the differentiation-inducing effect of 13-*cis*-RA, which is now becoming a standard modality for high-risk NBL cases [16]. Therefore, we examined the combination effect of 5-aza-dC and 13-*cis*-RA using a CIMP(+) NBL cell line, NB-39nu, which had methylation of 3 of the 4 target genes of the CIMP (*CYP26C1*, *FERD3L*, *CRYBA2* and *PCDHGC4*) and was reported to be suitable for analysis of differentiation induction [25].

A clear cumulative effect on the suppression of cell growth was observed (fig. 6a). Also, expression of a neuronal differentiation marker, neurofilament light polypeptide *(NEFL)* [26], was markedly induced when 13-*cis*-RA and 5-aza-dC were combined (fig. 6b). *CYP26C1*, a target gene of the CIMP, was also induced only when 13-*cis*-RA and 5-aza-dC were combined. Neurite outgrowth, a reliable marker for neuronal differentiation of NBL cells [16], was observed by treatment with 13-*cis*-RA only, but was prominent when both 13-*cis*-RA and 5-aza-dC were combined (fig. 6c). The number of cells that underwent apoptosis did not increase by the combination as shown by TUNEL assay (fig. 6d).

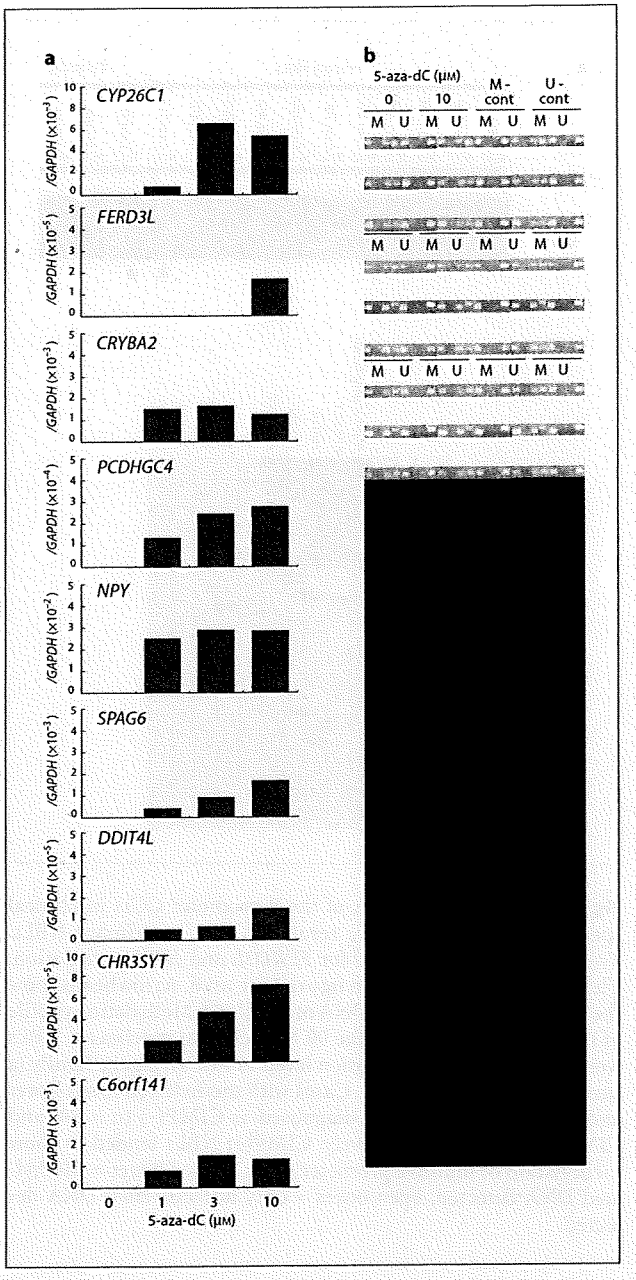

Fig. 4. Re-expression of the 9 genes by 5-aza-dC. IMR-32 cells were exposed to 0, 1, 3 and 10 μM 5-aza-dC on days 1, 3, 5 and 7, and DNA and RNA were harvested on day 8. Expression levels with each dose (**a**) and methylation status after exposure to 10 μM 5-aza-dC (**b**) were examined by quantitative RT-PCR and MSP, respectively. All 9 genes were found to be re-expressed with demethylation. M = Primers specific to methylated DNA; U = primers specific to unmethylated DNA; M-cont = fully methylated DNA; U-cont = fully unmethylated DNA.

Discussion

Promoter CGIs of 4 genes *(CYP26C1, FERD3L, CRYBA2* and *PCDHGC4)* were methylated at significantly higher incidences in CIMP(+) NBLs, and were considered as target genes of the CIMP in NBLs. Three genes *(NPY, SPAG6* and *DDIT4L)* were methylated with low incidenc-

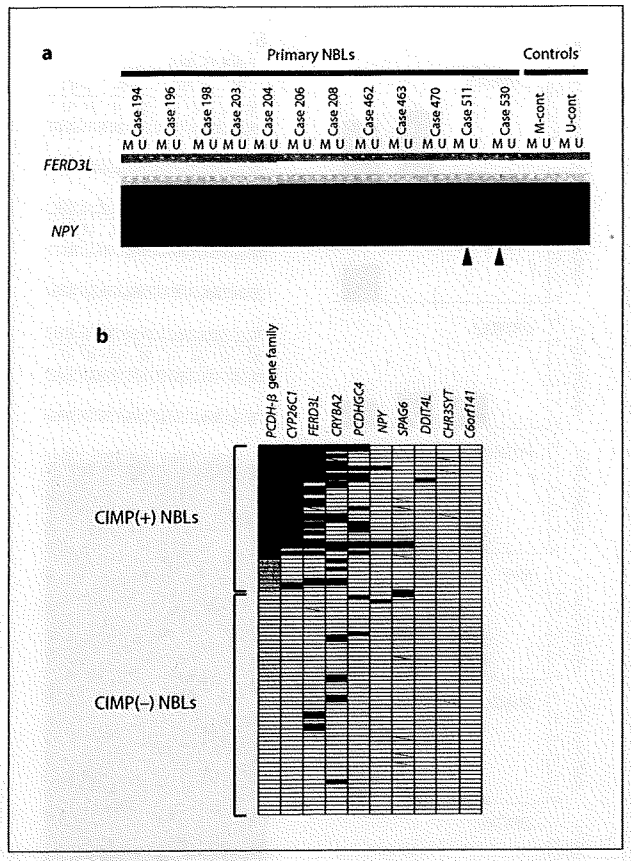

Fig. 5. Methylation analysis of the 9 promoter CGIs in clinical specimens. **a** Representative results of MSP in primary NBLs. Twelve cases were analyzed for *FERD3L* and *NPY* methylation. The same abbreviations as in figure 4 are used. Arrowheads show the presence of methylated DNA molecules. **b** Methylation profile of the 9 promoter CGIs in the 90 NBL clinical specimens. NBLs were aligned by the methylation levels of *PCDH-β* gene family (a surrogate marker of CIMP). Cases with methylation levels lower and higher than 40% were diagnosed as CIMP(–) (n = 54) and CIMP(+) (n = 36), respectively. CIMP(+) NBLs tended to show methylation of multiple promoter CGIs. Closed boxes = Methylated DNA detected; open boxes = only unmethylated DNA detected.

es in CIMP(+) NBLs, and were considered as candidate target genes. Except for *DDIT4L*, whose silencing had been identified in melanomas [27], silencing of these genes was a novel finding in any types of cancers. Although *FERD3L* and *PCDHGC4* were not expressed in the adrenal medulla, their expression in embryonal tissues and important roles in neuronal development have been reported [23, 28, 29]. This supported our hypothesis that CIMP affects various nonpromoter and promoter CGIs, that its presence is sensitively detected by methylation of nonpromoter CGIs and that its biological effects are exerted by methylation of promoter CGIs of various genes.

To support this hypothesis, the HRs given by methylation of each promoter CGI were calculated and compared with those given by the methylation of exonic CGIs of the *PCDHB* gene family (CIMP in NBLs). Only methylation of promoter CGIs of *CYP26C1* and *FERD3L* was significantly associated with prognosis, but the HRs given by these (12.3 and 7.2, respectively) were smaller than that given by the methylation of exonic CGIs of the *PCDHB* gene family (34.9). Even if the cases were limited to non-mass screening cases, the HRs given by methylation of promoter CGIs of *CYP26C1* and *FERD3L* (3.0 and 2.6, respectively) were smaller than that given by the methylation of exonic CGIs of the *PCDHB* gene family (10.9). These results indicated that exonic CGIs of the *PCDHB* gene family are consistently methylated in NBLs with the CIMP, while methylation of promoter CGIs still has a stochastic factor even in NBLs with the CIMP.

PCDHGC4 is a member of the *protocadherin-γ* gene family, which is deeply involved in neuronal maturation and brain development [28, 29]. One of the *protocadherin-γ* family genes, *PCDHGA11*, is reported to be silenced in astrocytomas [30]. FERD3L, also known as N-TWIST, is an evolutionarily conserved bHLH protein expressed in the developing central nervous system, and is an important regulator of neurogenesis [23]. *CYP26C1* is known to be involved in the development of the brain and the production of migratory cranial neural crest cells [31]. *NPY* encodes neuropeptide Y, a sympathetic neurotransmitter, which is expressed in differentiating NBL cells [32]. *CRYBA2* is a constituent of the lens, and the significance of its silencing is unclear [33]. These genes were methylated randomly in a fraction of CIMP(+) NBLs. Their silencing was considered to be involved in the poor prognosis of CIMP(+) NBLs, along with silencing of other unidentified genes.

Regarding the *protocadherin* gene families, nonpromoter CGIs of the *PCDH-α* and *PCDH-β* gene families (5q31) were found to be highly and consistently methylated in CIMP(+) NBLs, and their methylation levels were strongly associated with poor prognosis in NBLs. Here, it was found that *PCDHGC4* (5q31) was frequently silenced in CIMP(+) NBLs due to methylation of its promoter CGI. *PCDHGC4* is a member of the *PCDH-γ* subfamily C that contains 3 genes *(PCDHGC3, PCDHGC4* and *PCDHGC5). PCDHGC3* also has a CGI in its promoter region and was silenced in CIMP(+) NBLs (data not

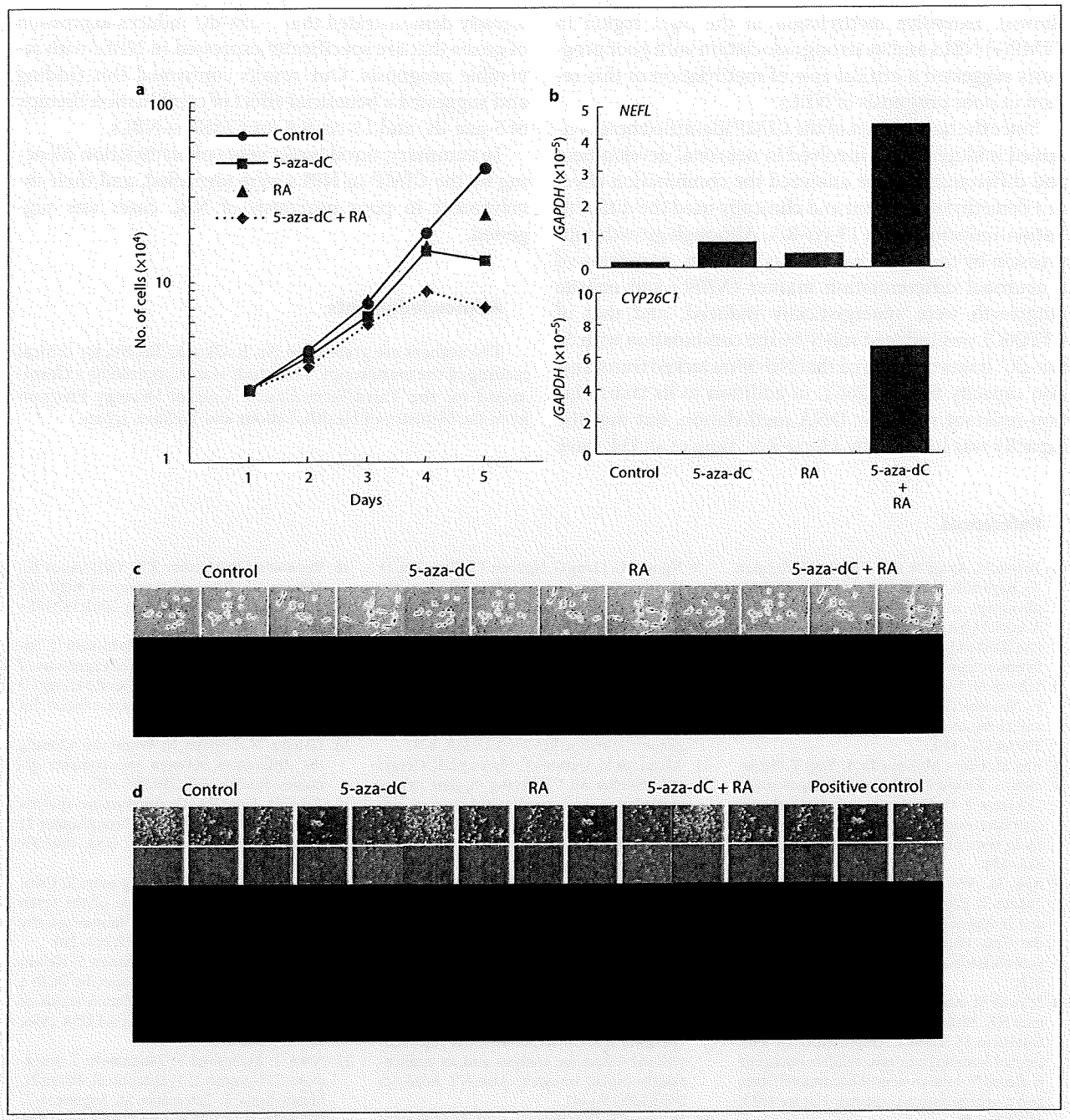

Fig. 6. Effects of the combination of a demethylating agent and 13-*cis*-RA on growth and differentiation of NBL cell lines. NB-39nu cells were treated with 5-aza-dC (1 μM), 13-*cis*-RA (1 μM) or their combination on days 1, 2, 3 and 4. Control cells were treated with PBS. RA = 13-*cis*-RA. **a** Effects on cell growth. Each analysis was performed in triplicate, and repeated twice. The average number of cells of the 2 analyses is shown. **b** Expression of a neuronal marker, *NEFL*, and a silenced gene, *CYP26C1*, on day 3, analyzed by real-time RT-PCR. Synergistic effects were observed. **c** Morphology of cells on day 5. Neurite outgrowth was observed after RA treatment, and was prominent after the combination. **d** Results of the TUNEL assay. No significant differences were observed on day 5.

shown). Extensive methylation in the 5q31 region in CIMP(+) NBLs and its strong association with poor prognosis suggested a critical role of methylation of this region in poor prognosis of NBLs.

Since the target genes of the CIMP identified here contained multiple genes involved in neuronal development and differentiation, we analyzed the combination effect of a demethylating agent and clinically used the differentiation-inducing agent 13-*cis*-RA. Although growth suppression by the combination was additive, expression of a neuronal differentiation marker *(NEFL)* and neurite outgrowth were synergistically induced, and that of *CYP26C1* was induced solely by the combination with 5-aza-dC. It was considered that NB-39nu lacked transcription capacity for *CYP26C1*, in addition to its transcription-resistant status by DNA methylation, but that the capacity was induced by 13-*cis*-RA. Tang et al. [34] have already demonstrated that 5-aza-dC induces expression of genes that are specifically expressed in NBLs with favorable prognosis. Our results confirmed this finding and suggested a beneficial effect of combination therapy of 5-aza-dC and 13-*cis*-RA for CIMP(+) NBLs.

In summary, novel target genes of methylation silencing by the CIMP in NBLs were identified, and their involvement in poor prognosis of NBL cases was suggested.

Acknowledgments

The authors are grateful to Dr. E. Okochi-Takada for critical reading of the manuscript. This study was supported by a Grant-in-Aid for the Third-Term Cancer Control Strategy Program from the Ministry of Health, Labour and Welfare, Japan.

References

1 Toyota M, Ahuja N, Ohe-Toyota M, Herman JG, Baylin SB, Issa JP: CpG island methylator phenotype in colorectal cancer. Proc Natl Acad Sci USA 1999;96:8681–8686.
2 Issa JP, Shen L, Toyota M: CIMP, at last. Gastroenterology 2005;129:1121–1124.
3 Schwab M, Westermann F, Hero B, Berthold F: Neuroblastoma: biology and molecular and chromosomal pathology. Lancet Oncol 2003;4:472–480.
4 Abe M, Ohira M, Kaneda A, Yagi Y, Yamamoto S, Kitano Y, Takato T, Nakagawara A, Ushijima T: CpG island methylator phenotype is a strong determinant of poor prognosis in neuroblastomas. Cancer Res 2005;65:828–834.
5 Abe M, Westermann F, Nakagawara A, Takato T, Schwab M, Ushijima T: Marked and independent prognostic significance of the CpG island methylator phenotype in neuroblastomas. Cancer Lett 2007;247:253–258.
6 Schwab M, Alitalo K, Klempnauer KH, Varmus HE, Bishop JM, Gilbert F, Brodeur G, Goldstein M, Trent J: Amplified DNA with limited homology to *myc* cellular oncogene is shared by human neuroblastoma cell lines and a neuroblastoma tumour. Nature 1983;305:245–248.
7 Brodeur GM, Seeger RC, Schwab M, Varmus HE, Bishop JM: Amplification of *N-myc* in untreated human neuroblastomas correlates with advanced disease stage. Science 1984;224:1121–1124.
8 Seeger RC, Brodeur GM, Sather H, Dalton A, Siegel SE, Wong KY, Hammond D: Association of multiple copies of the *N-myc* oncogene with rapid progression of neuroblastomas. N Engl J Med 1985;313:1111–1116.
9 Nguyen C, Liang G, Nguyen TT, Tsao-Wei D, Groshen S, Lubbert M, Zhou JH, Benedict WF, Jones PA: Susceptibility of nonpromoter CpG islands to de novo methylation in normal and neoplastic cells. J Natl Cancer Inst 2001;93:1465–1472.
10 Ushijima T, Watanabe N, Okochi E, Kaneda A, Sugimura T, Miyamoto K: Fidelity of the methylation pattern and its variation in the genome. Genome Res 2003;13:868–874.
11 Alaminos M, Davalos V, Cheung NK, Gerald WL, Esteller M: Clustering of gene hypermethylation associated with clinical risk groups in neuroblastoma. J Natl Cancer Inst 2004;96:1208–1219.
12 Alaminos M, Davalos V, Ropero S, Setien F, Paz MF, Herranz M, Fraga MF, Mora J, Cheung NK, Gerald WL, Esteller M: EMP3, a myelin-related gene located in the critical 19q13.3 region, is epigenetically silenced and exhibits features of a candidate tumor suppressor in glioma and neuroblastoma. Cancer Res 2005;65:2565–2571.
13 Kaneda A, Takai D, Kaminishi M, Okochi E, Ushijima T: Methylation-sensitive representational difference analysis and its application to cancer research. Ann NY Acad Sci 2003;983:131–141.
14 Ushijima T: Detection and interpretation of altered methylation patterns in cancer cells. Nat Rev Cancer 2005;5:223–231.
15 Ushijima T, Morimura K, Hosoya Y, Okonogi H, Tatematsu M, Sugimura T, Nagao M: Establishment of methylation-sensitive-representational difference analysis and isolation of hypo- and hypermethylated genomic fragments in mouse liver tumors. Proc Natl Acad Sci USA 1997;94:2284–2289.
16 Reynolds CP, Matthay KK, Villablanca JG, Maurer BJ: Retinoid therapy of high-risk neuroblastoma. Cancer Lett 2003;197:185–192.
17 Kaneda A, Kaminishi M, Nakanishi Y, Sugimura T, Ushijima T: Reduced expression of the *insulin-induced protein 1* and *p41 Arp2/3 complex* genes in human gastric cancers. Int J Cancer 2002;100:57–62.
18 Lisitsyn N, Lisitsyn N, Wigler M: Cloning the differences between two complex genomes. Science 1993;259:946–951.
19 Takai D, Jones PA: Comprehensive analysis of CpG islands in human chromosomes 21 and 22. Proc Natl Acad Sci USA 2002;99:3740–3745.
20 Kaneda A, Kaminishi M, Sugimura T, Ushijima T: Decreased expression of the seven ARP2/3 complex genes in human gastric cancers. Cancer Lett 2004;212:203–210.
21 Herman JG, Graff JR, Myohanen S, Nelkin BD, Baylin SB: Methylation-specific PCR: a novel PCR assay for methylation status of CpG islands. Proc Natl Acad Sci USA 1996;93:9821–9826.
22 Niwa T, Yamashita S, Tsukamoto T, Kuramoto T, Nomoto T, Wakazono K, Fujita H, Matsushima T, Tatematsu M, Sugimura T, Ushijima T: Whole-genome analyses of loss of heterozygosity and methylation analysis of four tumor-suppressor genes in *N*-methyl-*N'*-nitro-*N*-nitrosoguanidine-induced rat stomach carcinomas. Cancer Sci 2005;96:409–413.